Study of Etch Pits on Zinc Cleavages

A QUANTITATIVE STUDY
OF
ETCH MORPHOLOGY
OF
(0001) ZINC CLEAVAGES

By

DONALD DAVIE McAUSLAND, B.Sc. A.R.C.S.T.

A Thesis

Submitted to the Faculty of Graduate Studies

in Partial Fulfilment of the Requirements

for the Degree

Master of Science

McMaster University

August 1967

MASTER OF SCIENCE (1967)
(Metallurgy)

McMASTER UNIVERSITY
Hamilton, Ontario.

TITLE: A Quantitative Study of Etch Morphology of (0001) Zinc Cleavages

AUTHOR: Donald Davie McAusland, B.Sc. (Glasgow University)

A.R.C.S.T. (Strathclyde University)

SUPERVISOR: Professor M. B. Ives

NUMBER OF PAGES: viii, 86

SCOPE AND CONTENTS: The (0001) plane of zinc monocrystals were etched over a range of HCl/95% ethyl alcohol solutions for different etch times to produce etch pits. The etched surface was examined on the Zeiss interference microscope and from the interferograms made pits slopes, depths and rate of deepening were evaluated. The results indicate that the rate of widening of the pits formed is dependent on the defect causing the pit while the pit shape is governed by the HCl in the etchant.

ACKNOWLEDGEMENTS

The author wishes to thank Professor M. B. Ives for his advice, aid and encouragement which proved invaluable in the completion of this project.

Thanks are also due to Mrs. B. Baskin for help with experimental work and for her constant encouragement.

I also acknowledge the useful and stimulating discussions with my research colleagues Mr. W. Carson, Mr. P. C. Hancock and Mr. R. O. McElroy.

The work was performed with the support of the U. S. Office of Naval Research and the National Research Council of Canada.

The author gratefully acknowledges the receipt of a McMaster University Graduate Scholarship.

Table of Contents

List of Illustrations

Tables I, II, III	Show K' rate of pit widening θ' angle of pit side with (0001) d/t = rate of pit deepening for each etchant system for three pit types, with slopes around 5°, 2.5° and 1.5° respectively.
Figures 21 and 22	Opposite cleavage faces of specimen which has been scratched on outside.

Chapter I

Introduction

Most of the theories dealing with dissolution phenomenon and those dealing particularly with etch pit formation use microscopic concepts of monatomic steps and kinks and the subsequent bunching of steps into multiatomic ledges. This bunching of (steps or) ledges depends on the relative velocities of ledges emanating from the source, normally a dislocation and this in turn is determined partly by diffusion fields and partly by inhibition, the degree of control exerted by each depending on the system.

Hulett and Young (45) tested the theory relating to ledge bunching and stability model by a computer programme and obtained good correlation with their experimental finding with pit formation in electro-etching of copper monocrystals.

The most common technique used for examination of etch pit detection has been by the optical microscope generally with low magnification. Many of the workers in the field of etch pitting have been most interested in producing visible pits in the surface of metals. The pits formed appear frequently in published work as lines of dots and these are correlated with emergent dislocations. If the correlation can be established and the technique found to be reproducible, this can be extremely useful to the mechanical metallurgist in determination of dislocation distributions and densities. The etch pit method can be extremely sensitive to small stresses and has the advantage of being non-destructive. The technique has been used by Gilman et al (44) on

LiF to study dislocation velocities and in metals the determination of lines of pits has been used to identify the operative slip systems under specific deformation modes. However, for these experiments "fresh" dislocations must be etched and the pits at "fresh" dislocations in metals tend to be shallow.

Some work has been done using the interference microscope to study the etched crystal surface, both on ionic and metal surfaces. This has the advantage over optical techniques in that a quantitative approach may be used to examine pits shapes, depths, and slopes. This is a macroscope tool for the study of surfaces. When the instrument is appropriately adjusted, points of equal height are joined by a fringe (c.f. geographic contours). Thus a conical pit would have the appearance of concentric circles. Thus by this technique a microscopic picture of the pit morphology can be obtained. Due to the distance between fringes it is impossible to detect the arrangement of ledges. To be able to detect ledge spacing step heights and regularity of pit morphology the techniques of electron microscopy must be employed. Replication techniques have been used in the study of inhibition effects on LiF etching in this laboratory by Ramachandran and Ives (17) but the technique is not yet being widely used though attempts are currently in progress to apply the technique to the study of etched zinc surfaces.

In this study an attempt was made to quantitatively measure pit parameters such as depth rate of deepening, pit slope and pit shape on the basal plane of zinc with different concentrations of HCl in 95% ethanol - the Rosenbaum and Saffren (23) etchant - but using a greater range of HCl concentrations than employed by those workers.

FIGURE A

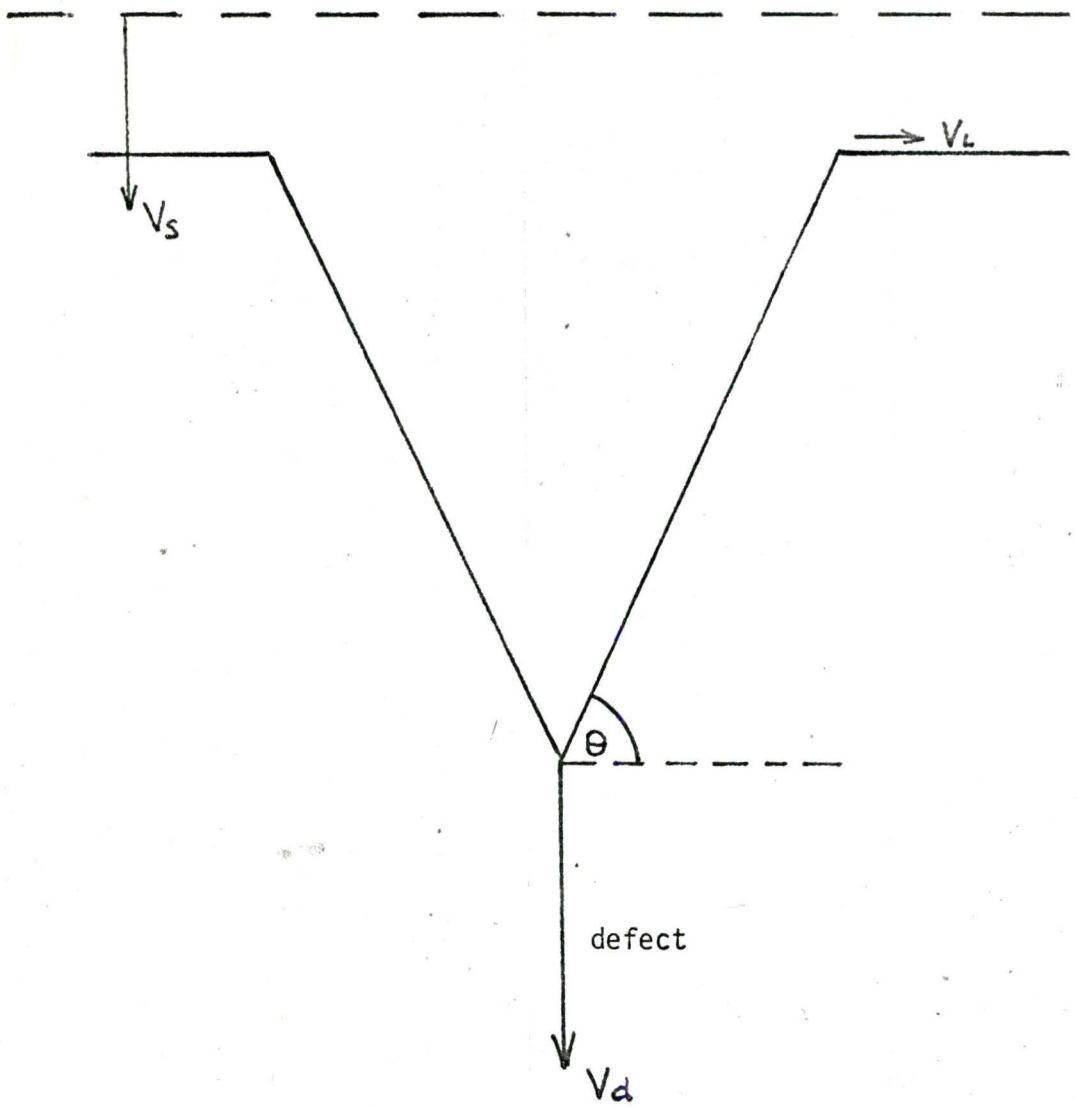

V_d ≡ velocity of deepening at defect

V_s ≡ velocity of lowering of (0001) plane

V_L ≡ lateral velocity of pit sides

θ ≡ measured angle from pit profile - θ' x constant

It was the aim of this work to study the effect of etchant concentration and etchant time on pit morphology. Fig.A represents a pit.

It is considered that the macroscopic pit morphology is determined by

$V_s \equiv$ velocity of lowering of the (0001) plane

$V_L \equiv$ lateral velocity of pits sides, i.e. velocity of widening

$V_d \equiv$ velocity of dissolution at the defect

$\theta' \equiv$ true angle the pit makes with the (0001) plane close to the defect

$$\tan \theta' = \frac{V_d - V_s}{V_L}$$

$$= \frac{(d/t)_d - (d/t)_s}{V_L}$$

$d \equiv$ pit depth, microns

$t \equiv$ etching time, seconds

$d/t \equiv$ rate of deepening of the pit

Assume $(d/t)_s$ is constant for all pits. Then

$$V_L = \frac{(d/t)_d}{\tan \theta'}$$

V_L can be calculated experimentally and has been designed as K'.

It is not the aim of this study to identify the defects which cause pitting, though subsidiary experiments were performed in an attempt to be able to make meaningful estimation of the defects responsible for etch pitting.

Matched cleavage faces were etched and examined for correspondence of pits. Specimens were deformed by scratching to ascertain if

the concentration of deep pits increased, and specimens were deformed at elevated temperatures in an attempt to introduce screw dislocations from the prism plane and the sample cleaved and etched to examine the distribution of pits.

Several specimens were subjected to successive etching experiments where the same pits on the surface were photographed at successively longer etching times, in the same etchant. Plots of depth of the pit versus etching time could be drawn to examine the relationship between pit depth and etching time. This procedure was repeated for several HCl concentrations and a single concentration of HBr. If the rate of widening of the pits associated with different defects is assumed to be constant, then K', which is physically a measure of this parameter, will be constant for etch pits arising from different defects on the same crystal face under constant etching conditions. Thus the growth of the etch pits will be dependent on the defect.

The value of K' was examined for the pits associated with these defects for different etching times and at different etching concentrations in order to check the hypothesis that K' is a constant, during pit growth, and for pits formed by etchants of different concentrations.

Chapter II

Literature Survey and Theory

Before considering the more specific problems associated with the formation of etch pits on specific crystal faces and particularly metal faces, the various theories relating to crystal dissolution will be briefly reviewed. Following Kossel (1) the initial crystal interface is considered to be in the form of a series of ledges on which are kinks of monomolecular offset. Dissolution occurs by the removal of atoms from the self-perpetuating kink and as a kink travels along a step the step is eliminated and recedes by one atomic dimension.

Kinks are nucleated on this ledge and the process repeated until the ledge is removed from the surface. Since the general surface of a crystal is considered to be composed of kinked ledges the process is simultaneously occurring across the whole surface, general dissolution occurs and a microscopically flat surface is obtained. Crystal edges always provide a source of ledges but in large crystals the effect of dissolution at the crystal edges is negligible.

The theories outlining general surface dissolution are those of Frank (2) - the topographical or phenomenological theory - and that of Burton, Cabrera and Frank (B.C.F.) - the mechanistic theory (3). The B.C.F. theory and later modifications (4-6) equate diffusion fluxes around ledges and kinks to the planar diffusion flux through the stagnant layer and obtain equations with ledge velocity dependent on ledge spacing.

It is not proposed to restate these theories in detail. The Frank theory has been quantitatively applied to macroscopic dissolution of Ge and LiF crystal surfaces by Ives (7, 8) but problems are encountered when either theory is rigorously applied to dissolution by formation of etch pits, when an inhibitor is present in solution.

For the mechanistic theory to apply, even in the simple cases kinked steps must exist on the surface and the undersaturation of the solvent must be such that the kink atom is removed from the solid. Nucleation of fresh kinked steps is required and the undersaturation at the surface must not be less than a critical value otherwise equilibrium is attained.

Kinked steps can also occur by nucleation of monomolecular pits on the otherwise perfect surface. A factor producing the pit is the undersaturation of the solvent. The sites where these monomolecular pits are nucleated are generally associated with a defect in the surface which reduces the (activation) energy for nucleation. The monomolecular pit on say a crystal with four fold symmetry has four ledges each normal to each other and the ledges move outwards from the source as before. The topographical and B.C.F. theories and that of Hirth and Pound (5) for evaporation from metal surfaces predict the manner in which these ledges move away from the source and the acceleration of ledges and time to reach steady state velocities largely determine the morphology of the pit. That is, if the steady state velocity is immediately operative the slope at the source which is determined by the B.C.F. theory [modified and leading to a solution similar to that of Hirth and Pound] will remain constant. If the ledges accelerate the slope will

become less steep as the ledges move further from the source, until the steady state ledge velocity is reached.

Gilman et al (9) suggests that the rate of solution in chemical polishing is limited by the rate of nucleation of unit pits. The initial nucleation sites deepen and produce more ledges which move away from the source. Thus after continued dissolution the surface should consist of a series of wide shallow (saucer-like) depressions on the surface of the crystal. This has been found to be the case for dissolution of LiF by pure water (9).

Etch pit formation consists of two stages:

1) nucleation of monomolecular steps.
2) motion of steps away from the source.

These two processes are not mutually independent, being related by the presence of diffusion fields, the solution of which is difficult.

Nucleation of Steps

It is agreed that the initiation of an etch pit is a nucleation process. This is borne out by the fact that pit nucleation is highly dependent on the undersaturation of the solvent and high undersaturations are required to produce pitting.

According to the treatment of the problem by Cabrera and Levine (4) the activation energy for nucleation of a pit is less for the site of an emergent dislocation than a site on perfect crystal surface. This is so because of the region of high energy around a dislocation. However this energy difference only becomes important at high undersaturations.

To deal with the problem quantitatively some measure of this extra energy around a dislocation must be computed. An example where this can be done with some accuracy is a "fresh" edge dislocation.

Here the extra energy is written as

$$\omega_{(r)} = \tau b^2/2\pi \ln r/r_o = \frac{\tau b^2}{2\pi} \ln r/a + \omega_{(c)} \qquad (1)$$

$\omega_{(r)}$ ≡ extra energy per unit length contained in a cylinder of radius around a dislocation

$\omega_{(c)}$ ≡ core energy of the dislocation

τ ≡ some combination of elastic constants

b ≡ Burgers vector of the dislocation

r ≡ radius of cylinder of material around the dislocation

r_o ≡ a length ($\sim 10^{-8}$ cms.) chosen so that $\omega_{(c)}$ represents the non-elastic (core) energy

a ≡ the nearest neighbour distance in the crystal

The first portion of the equation $\frac{\tau b^2}{2\pi} \ln r/a$ represents the elastic energy of the dislocation while $\omega_{(c)}$ represents the core energy on which it is difficult to place a numerical value. This expression has been found to satisfy atomic calculation for an edge dislocation in NaCl lying in the (110) plane with b = $\sqrt{2a}$ <110>.

From equation (1) can be shown that there exists a critical undersaturation below which there is no barrier (no activation energy required) to nucleate a pit at a dislocation. With a saturation concentration Ce for a particular solute in contact with a dilute solvent the critical undersaturation Co/Ce is obtained from

$$\ln Ce/Co = \frac{\pi^2 \gamma \Omega}{kT\ b^2\ \tau} \qquad (2)$$

Ce ≡ saturation concentration of solvent

Ce/Co ≡ the critical undersaturation for pit nucleation

γ ≡ surface energy of the edge of the step

Ω ≡ molecular volume

k ≡ Boltzmann constant

T ≡ temperature °A

Ce/Co can be found experimentally and reasonable values of the surface energy inserted. Thus the radius of the critical nucleus is calculated as

$$\rho = \frac{\tau b^2}{2\pi\ \gamma}$$

ρ ≡ radius of critical nucleus.

For an edge dislocation spontaneous nucleation occurs while for a screw dislocation a similar calculation can be carried out in which case the step associated with the emergent screw dislocation winds itself into a spiral of critical radius.

From this it is calculated that the extra energy at an edge dislocation is approximately one half elastic and one half core energy. Cabrera and Levine considered this approach satisfactory for the etching of ionic crystals in dilute solvents. The elastic energy component is considered to produce an electrochemical effect as between strained and strain-free areas of the surface.

Gilman (10) disputes the Cabrera-Levine suggestion about the extra energy of the dislocation. He suggests that only the core energy of the dislocation contributes to the activation energy for

nucleation and supports his contention with examples.

Gilman further suggests that it is the low core energy of dislocations in metals relative to ionic compounds which makes nucleation of dislocation etch pits in metals more difficult. This assertion is important when it is known that the elastic strain energies of dislocations in metals are as large if not greater than in ionic crystals.

Motion of Steps

Once a step has been nucleated it moves away from the source as the solid dissolves and in so doing reduces the undersaturation in the vicinity of the source, thereby making the nucleation of the next step more difficult.

In moving away from the source the step introduces more and more solute into solution and to allow the second step to be nucleated at the source the radius of the step centred on the dislocation must become large relative to the depth so that the undersaturation at the source reaches the critical value for further nucleation. This results in a very shallow pit of large lateral dimensions; in fact to what amounts to a flat surface. For this case with no inhibition V_L is large and V_d is small; $\tan \theta'$ is small. Cabrera and Levine then consider the case where the nucleated steps are locally "poisoned" or inhibited. The adsorbable impurities in the solution will reduce the radius of curvature of the step. This reduction will be entirely dependent on the spacing of the impurities adsorbed on the ledge. Therefore the ledge is slowed down and in the limit stopped. The concentration of the dissolved solid will be reduced in the neighbourhood of the dislocation

and nucleation of further steps becomes much easier. Cabrera (11) feels that this mechanism of impurities producing high local curvature of the ledge is most important in slowing up ledge motion as opposed to impurities on kink sites and having the same effect.

Gilman, Johnston and Sears (9) proposed a different theory for slowing ledge motion by inhibition. Gilman et al. suggest and his theory is largely accepted at least for ionic crystal dissolution, that a specific inhibitor must be present in solution which adsorbs and more probably chemisorbs at kink sites on the moving ledge thereby slowing up ledge movement and reducing ledge velocity. Thus microscopically the Gilman et al. and Cabrera-Levine theories have the similar effects of slowing ledge motion but the atomic mechanism by which this is achieved is different.

Dissolution of LiF

A considerable amount of the theoretical work on dissolution has been done on lithium fluoride. This subject will be briefly outlined as an example of the parameters involved and the effect of different conditions and conclusions drawn therefrom.

Gilman, Johnston and Sears exhaustively tested a large number of compounds in the solvent to determine what ingredients were active as inhibitors. They found that the anion was relatively unimportant and that only Fe^{+++} and Al^{+++} were effective cations. They decided that a cationic inhibitor had special properties which were important:

(a) valence of cation

(b) size of cation

(c) stability of its fluoride salt

(d) low solubility of its fluoride salt

(e) stability of its fluoride complex.

In summary the most effective cations are within 25% of the size of the lithium ion, they have a stable fluoride complex.

For most studies of etch pit formation in LiF (12, 13, 14) a dilute aqueous or acidic etch was used with a small concentration of Fe^{+++} ion solution in the form of ferric fluoride.

With no Fe^{+++} ion present very shallow indistinct pits are formed. With addition of Fe^{+++} ion square pits are formed, the depth and orientation of which vary with the type of defect etched-screw, edge dislocation, fresh, decorated dislocation and type of etchant, aqueous or acidic. The orientation is determined by the etchant and the pit depths by dislocation types.

As the Fe^{+++} ion concentration is increased the pits become deeper and width/depth ratio decreases up to the optimum Fe^{+++} ion concentration. Beyond this concentration the pits begin to barrel and eventually become conical with increasing Fe^{+++} ion concentration.

The pit deepening up to the optimum is considered to be time dependent adsorption (Ives and Hirth) (13) with the more slowly moving ledges being more efficiently poisoned. As the ledges are more efficiently poisoned ledge motion is slowed, while nucleation rate is unaffected and so pit slope increases. At the optimum Fe^{+++} ion concentration (small square pits) monokink coverage was considered to occur. However, work by Ramachandran and Ives (15) suggests this hyphothesis is unlikely. With iron concentrations greater than the optimum when the pits begin to round Ives and Baskin (16) suggest that

complexes in solution begin to play a dominant role in the etching by affecting the diffusion control.

Ramachandran and Ives (17) found in an electron microscope study that the pit squareness was maintained at the pit centre and suggest that ledges close to the source have less inhibitor associated with them making it more difficult to form the species which increases the diffusion barrier to material being removed from the pit.

By reducing the undersaturation, i.e. increasing the LiF concentration in the solvent the pit slope can be increased. The undersaturation can be decreased to a critical value above which no pit nucleation occurs. The decreasing undersaturation decreases the dissolution rate thus allowing more efficient poisoning of the kink on the ledges and thereby slowing ledge motion and causing increased pit slope.

Solute segregation to dislocations in LiF tend to reduce the pit slope and depth. This is due to the impurity atmosphere reducing the local energy of the dislocation.

For best pitting conditions at reasonable undersaturations low surface energy and large shear modulus are desired. This is the case with ionic crystals and etch pits are most easily formed in these compounds.

The foregoing has dealt briefly with the microscopic theory of dissolution and dislocation etch pitting mainly with respect to ionic materials. Etching of metals will now be discussed.

Metal Etching

Etching is a term which is used very loosely, especially when applied to the dissolution of metals. Etching can be taken to mean the following:

(a) Cleaning the surface of the crystal. This should be more properly termed polishing.

(b) Surface dissolution to aid orientation determinations. Here etching or polishing is used to remove damaged surface layers prior to X-ray examination. Optical techniques can be used when etchants preferentially attack specific planes, producing different texture on the different crystallographic planes. Honess (18) and others in the 19th Century etched mineral crystals and were able to determine specific crystal planes by the shape of the etch figures on them.

(c) Metallographic etching is used mainly to show grain boundaries, precipitates, second phases on mechanically or electropolished surfaces.

(d) Etching may be used to study crystal imperfections especially dislocations intersecting the surface by the production of etch pits on the surface (46-53).

Of these only the latter (d) is of direct interest in this thesis and the term etching will be considered to be the dissolution process producing pits on the surface at the sites of crystal defects.

Etching processes which may be categorised in terms of the type of reaction between the etchant and the metal as follows (19).

(1) Chemical: this is an electron transfer process, the surface atoms undergoing a chemical change. Only reactions that form a product

which is removed can be employed.

(2) Electrolytic: The specimen is biased anodically to cause ions from the solid to pass into an electrolyte.

(3) Thermal: This involves vapourisation of atoms from the surface generally under conditions of both elevated temperature and undersaturation in the vapour phase.

(4) Solvation: A liquid which is a solvent for the solid is used, generally the solvent being undersaturated. This is akin to (3) except that the phase change is solid to liquid instead of solid to vapour.

(5) Cathodic Bombardment or sputtering: Here the energy of bombarding atoms from an emitter physically drives atoms from the solid surface.

(6) Alloying: This is rather similar to chemical etching except that a molten metal is used as the environment and a molten alloy is the product.

Generally only (1) to (4) are commonly used and thermal etching (3) is a different though related field of study from that undertaken in this work. Solvation (4) is commonly used in the etching of ionic crystals and the aqueous etch with ferric ion additions in LiF etching is an example of this technique.

Thus (1) and (2) are the most common methods of etch pit production in metals and in the present study only (1) is employed. F. W. Young et al. (20) on exhaustive studies of copper have used (2), electrolytic techniques, almost exclusively.

Faust (19) classified etchants into these types:

(a) Preferential: The etchant produces pits whose facets have a definite

crystallographic orientation.

(b) Non-preferential: The etchant not only produces a polished surface but also reveals (dislocation) etch pits.

(c) Polish: The etchant (polishant) produces a microscopically smooth surface with perhaps only grain boundaries being observed.

Thus (a) and (b) are the types of etchants which are used in the study of surface imperfections, principally dislocations.

Etch Pits on Metals

The extent of etch pitting on the surface of a metal depends to a large extent on the condition of the metal surface. The surface to be etched may be obtained in the following ways: cleavage of brittle materials, mechanical or electropolishing, and acid cutting include some of the common techniques. Faces of naturally grown crystals may also be etched directly though this is uncommon in metals.

As a smooth surface is etched with either a preferential or non-preferential etch, attack is initiated at discrete points on the surface causing pits to be formed. Although surface nucleation occurs a large pit does not always form at all points except under special circumstances. As in ionic crystals, surface nucleation requires that a nucleation barrier must be overcome and unless surface heterogenities are present dissolution will be slow. Such heterogenities include

(1) dislocations from the bulk crystal intersecting the surface,

(2) mechanically induced dislocations introduced by surface preparation,

(3) cleavage or growth steps,

(4) vacancies or vacancy clusters,

(5) precipitates,

(6) a discontinuous oxide or surface layer or layer of variable thickness or perfection.

Nucleation of monomolecular pits on close packed surfaces has been discussed mainly for the case of ionic crystals. It is considered that a similar mechanism is applicable on metallic surfaces at the points of emergence of crystalline defects. However, it has been found more difficult to produce etch pits on metallic surfaces. It is argued that it is more difficult to nucleate pits on metallic surfaces due to the lower core energy of the dislocation and lower surface energy and Vermilyea (21) suggested that it is not possible to produce pits in metals without prior segregation of impurities to dislocations. Vermilyea (21) suggests that the undersaturations required to nucleate pits on metal surfaces is extremely high. However, this nucleation is a case of solvation of a metal and not chemical etching where undersaturation considerations are of much less importance. Work by F. W. Young et al. on electrolytic etching of copper suggests that no prior segregation of impurity is required to produce measureable etch pits. In metal etching there is considerable doubt as to whether the difficulty in producing measureable etch pits is a function of the nucleation or the growth of the pit. The evidence tentatively suggests that in chemical etching of metals the controlling factor in pit formation is the retardation of growth or ledge motion, after nucleation. Though that prior segregation of impurities to dislocations makes production of etch pits easier is widely accepted, it appears that it is not necessary for production of measureable pits in all metal/solution systems. The impurity

segregation to a dislocation tends to reduce the core energy of the dislocation but often increases the chemical reactivity. Thus the effect of the atoms segregated at dislocations would appear to be electrochemical in nature.

Vermilyea (21) has proposed that in certain circumstances pit formation is due to the formation of an oxide film, present either before etching or actually produced by the etchant. He found that in the etching of germanium and silicon with HF/HNO_3 mixtures that different pit shapes were produced when the HF/HNO_3 ratios were altered. He concludes from this that the dislocation alters the oxide layer mechanically or alters its conductivity allowing attack to proceed more rapidly at the points of emergent dislocations. Thus the form of the oxide formed on the surface has an effect on the etch pitting characteristics of the metal.

However, in other systems (22) it is found that though etch pits can be formed on freshly cleaved surfaces, no pits, or a surface covered with micropits, are formed when the specimen is re-etched after electropolishing or chemical polishing. The polishing is considered to cause a surface film to be formed which interferes with pit formation. Thus Vermilyea's assertion that etch pits in metals can only be formed by:

(a) dislocation "decoration"

(b) formation of an oxide film which protects the bulk surface must be viewed with considerable doubt.

It is also suggested that the solvent may contain surface active agents which adsorb on the surface reducing general surface

dissolution but leaving attack at dislocation/surface intersections unaffected.

Thus at present it is impossible to state rules for production of etchants which will cause dislocation etch pits to form in metals. The most plausible suggestion is the analogy to solvation of ionic crystals. Thus increased reactivity of the surface at the defect causes accelerated chemical attack there and some ingredient in the etchant acts as an inhibitor slowing up the motion of the ledges from the defect source. F. W. Young (37) found that Br^- ion in copper dissolution, reduced the general dissolution rate as did Fe^{+++} ion in dissolution of LiF and he suggested that etch pits were formed by enhanced chemical attack at the dislocations, bromide ion acting as a ledge "poison".

Pit Morphology

The trace of the etch pit generally reflects the symmetry of the etched surface but the orientation of the pit sides are generally determined by the etchant employed. For example Gilman et al. (9) produce pyramidal pits on the cleavage face of LiF but the orientation of the sides depends on whether the "acidic" or "aqueous" etchant is used. Similarly, Rosenbaum and Saffren (23) produce hexagonal pits on zinc cleavages but depending on whether HCl or HBr is an etchant ingredient the orientation of the sides of these hexagons differs.

Studies on germanium dissolution (24) indicate that the oxidising agent apparently determines the plane which is preferentially attacked while the complexing agent affects the rate of attack. However,

FIGURE B

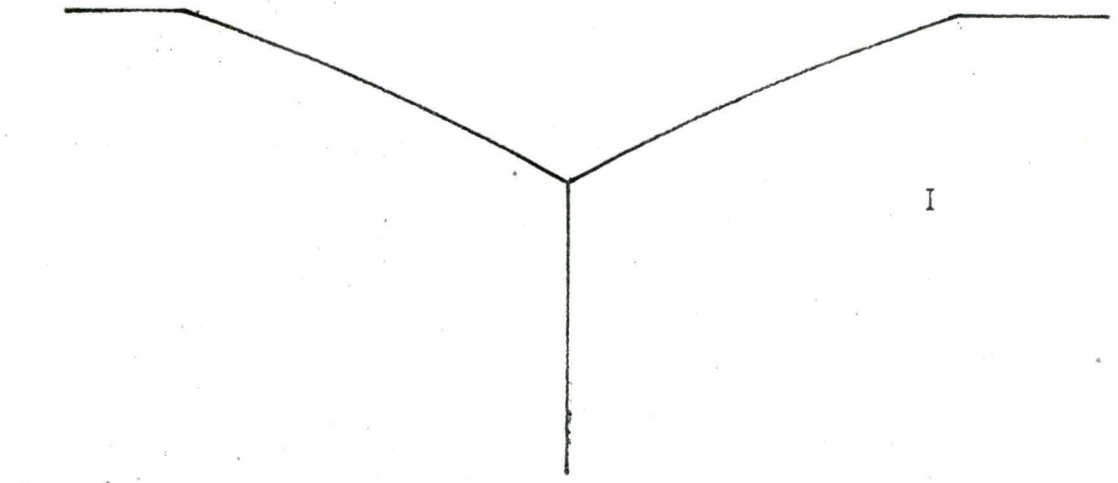

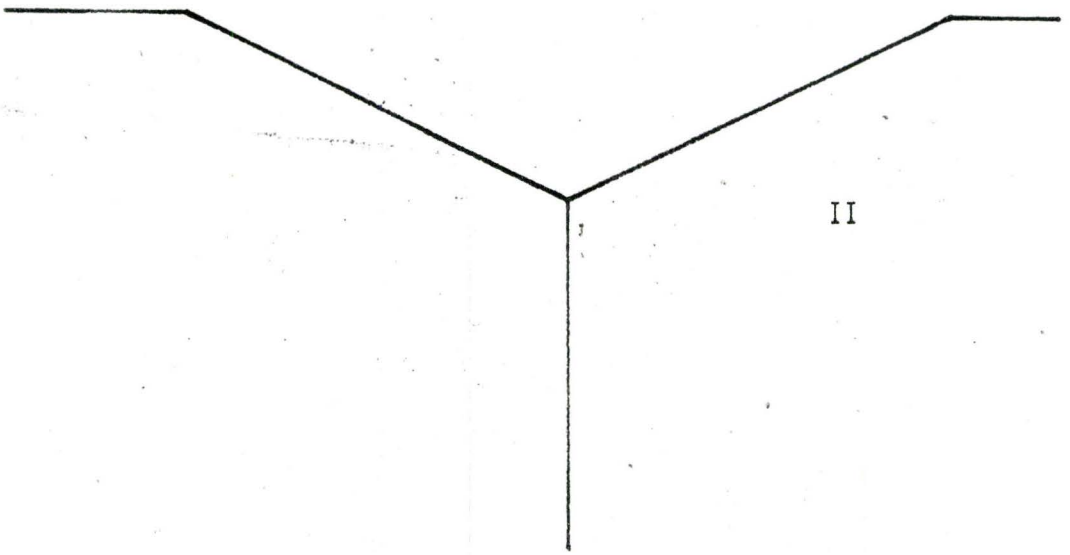

the planes acted upon preferentially are not always determined by the oxidant if this is the hydrogen ion. In the case of the halogen acids the anion appears to determine the pit morphology.

Faust (19) suggests that the pit morphology is dependent on whether preferential or non-preferential etchants are used.

He suggests that etching with a non-preferential etchant produces a pit with curved sides (Fig. B), the pit generally being conical. The degree of offset between the base of the cone and the centre of the surface contour indicates the angle the dislocation makes with the surface. Faust suggests that prolonged etching with a non-preferential etchant makes the pit flat bottomed and eventually eliminates it.

Faust suggests that preferential etchants produce pits which reflect the crystal symmetry. He further suggests that etching some planes produces smooth straight sides while etching other faces produces macroterracing the degree of macroterracing depending on the relative rate of attack on the planes revealed.

Production of Etch Pits from Defects Other than Dislocations

Mechanically induced dislocations produced either intentionally by abrasion or formed in the course of specimen preparation are generally in the form of shallow dislocation loops. The pits formed tend to be obliterated quite rapidly especially if general surface attack is rapid. In addition, such dislocations are usually fresh - impurity segregation free - dislocations at which it is generally more difficult to produce pits on etching. There is also the possibility that the

products of abrasion become imbedded in the specimen surface prior to etching and these foreign particles may themselves give rise to etch pit formation.

Vacancies and impurities in the surface can nucleate monomolecular pits but unless these form vacancy clusters or impurity particles the pits nucleated will not form pits of observable size. Numerous workers in the study of etching have associated the large number of small pits on the crystal surface with vacancy clusters (25). The concentration of these will largely depend on the equilibrium concentration of vacancies at the melting point of the metal, on the rate of cooling and the concentration of dislocations which will act as vacancy sinks. Pitting associated with vacancy clusters has been found in irradiated crystals though whether these are true vacancy clusters on fission tracks is questionable. As an example Steadman and Pugh (26) using interferographic techniques measured pits in natural cronstedtite ($Fe^{2+}(Fe^{3+}Si)O_4(OH)_5$) crystals. These pits were claimed to be dislocation etch pits. This view was later challenged (27), the suggestion being that the pits measured were trails of fission fragments.

Impurity precipitates may be especially effective in producing etch pits when the impurity forms in filamentary precipitate. In both the case of vacancy clusters and impurity particles the pit ceases to deepen when the defect is removed by sufficient etching and the pit becomes flat bottomed.

Many metal surfaces are readily covered by a surface layer generally an oxide. This layer may vary in thickness and perfection and weaknesses in the layer may be breached before the general metal

surface is exposed allowing pitting to occur at imperfect points in the oxide layer which may bear no relation to the crystalline perfection of the underlying metal surface.

Induction period for pitting should occur if there is a measureable time for the protective (oxide) layer to be removed by the etchant.

Etching of Zinc

The early work on the etching of zinc was done by Meleka (28) on the cleavage plane of zinc using a solution of iodine in alcohol. He claimed that the pits formed were the sites of emergent dislocations. Meleka used high purity zinc suggesting that the pits form at "clean" dislocations.

Regel and Stepanova (29) repeated the work of Meleka and found that distinct etch pits could be formed on the basal plane if freshly cleaved surfaces were etched. However, after polishing and further etching quite different arrangements and even shapes of pits were observed. They concluded the etching technique of Meleka to reveal dislocations was unreliable.

Gilman (30) used an etchant (CrO_3, Na_2SO_4, H_2O) to produce etch pits on the basal plane of zinc. However, prior introduction of 0.1% cadmium into the zinc and an annealing treatment were required to produce pits. Thus Gilman after two years of intensive work on zinc etching required "decorated" dislocations to produce etch pits on the cleavage plane of zinc.

Regel et al. (29) attempted to reproduce Gilman's work on

zinc monocrystals but were unsuccessful. They attributed this to their specimens being high purity zinc and that Gilman's etchant could only be used to reveal "decorated" dislocations.

Regel et al. (29) used electroetching techniques on zinc crystals. Their etching solution was 33% H_3PO_4 + 67% C_2H_5OH. This solution can be used for electropolishing as well as etching, depending on the current density employed, the lower current density producing etch pits. However, after etching followed by electropolishing and then re-etching, the original arrangement of pits does not reappear. Thus this method of etching is not considered to be reliable. It was found that the etching (pitting) behaviour depended on the dissolved zinc in the electrolyte, more distinct pits appearing when some dissolved zinc was present, as opposed to a zinc free electrolyte. Zinc concentration was found to be difficult to control.

Regel et al. report trying various other etchants including H_3PO_4, HCl, HNO_3, H_2SO_4 and HF and in many cases pits were formed but results were found to be not reproducable. They suggest that pits are formed at surface defects other than dislocations. It would also appear that each etchant used was selective in the type of defect attacked.

Regel et al. then studied the case of weak etchants on the basal plane of zinc viz tap water. Tap water caused the formation of distinct six pointed star shaped pits. These could be matched on the opposite faces of the cleavages and the authors tentatively suggest that the pits are the result of the cleavage process, possibly dislocation loops. Subsequent etching with strong etchants eliminate these pits and attack the surrounding crystal surface. Thus the weak etchants show

pits which the strong etchants cannot reveal.

The experiment was repeated and each time the tap water analysed. It was found that slight variations in the water purity had a marked effect on the structure and distribution of etch pits. For example, the appearance of the surface etched in tap water in the winter period was quite different from that etched in the spring due to different impurity content of the water. The authors were unable to identify the constituents of the water responsible for this behaviour. Regel et al. suggest that the etch figures reflect both the symmetry of the crystal and the nature of the defect. However they do not feel confident enough to state which defects are responsible and caution the reader about assuming that etch pits are necessarily the sites of emergent dislocations.

Sharp (31) etched the basal plane of zinc monocrystals in the Gilman and De Carlo (32) zinc chemical polishing solution (Cr_2O_3, Na_2SO_4, H_2O) for times from 2-5 seconds. Sharp found that a fresh cleavage face was necessary to produce pits. He obtained his cleavage faces by bending the specimen at room temperature, since he found that cleaving the crystal at liquid nitrogen temperatures produced large unetched areas.

Sharp produced hexagonal pits with a good but not exact correspondence on opposite cleavage faces. He suggested that room temperature recovery of zinc may have been a factor in his not obtaining a one-to-one correspondence on opposite cleavage faces. He also detected assymmetrical as well as symmetrical hexagonal pits. These etch pits were considered to be sites of dislocations from pyramidal and prism

planes respectively, intersecting the (0001) plane.

No indication, however, is given of the depths of the pits and the short etching times used make this etchant system rather inflexible.

R. C. Brandt et al (33) conducted etching experiments on several planes of zinc and introduced a novel method of decorating dislocations. The crystal face is doped with mercury from $Hg(NO_3)_2$ solution and polished in the Gilman polishing solution. Instead of pits being formed at dislocations, pips, i.e. small hillocks, are formed and the authors consider that a one-to-one correspondence between pips and dislocations is obtained. Experiments were conducted with Hg^{197}(3%) and autoradiographs showed that the mercury concentrated at the dislocations. It is believed that the mercury moves rapidly over the surface to dislocation sites though whether the driving force for mercury surface diffusion is to reduce the strain energy of the dislocation or perturbation of the lattice field or both is not clear. Diffusion of mercury into the bulk crystal is negligible. Thus after introduction of mercury to the surface, with subsequent polishing the dislocation is more noble than the general surface which is attacked and the dislocation sites appear as hillocks. This technique has the advantage, for the mechanical metallurgist, in that the dislocations can be decorated after deformation treatments, whereas normal methods of decoration of dislocations by doping and annealing drastically alter the mobility of the impurity decorated dislocation. The paper also adds weight to the argument that solute decoration of dislocations subject to dissolution studies is electrochemical in nature. Thus if different impurities are

segregated at similar dislocations different rates of attack at the dislocations should result during etching under the same conditions. It was found that at surface misorientation of greater than approximately 5° the pips were difficult to see, suggesting that the angle between the side of the pip and the general surface is in the order of 5°.

George (34) etched the basal plane of zinc in Superoxol (one part 30% H_2O_2, one part 40% HF, four parts H_2O) producing star shaped symmetrical etch pits. The star shape of the pit gradually changes to regular hexagons towards the centre. The pits are made up of regularly spaced small terraces. George interprets the pits to be fresh dislocations of a screw character from the prism planes, and considers them to be associated with the growth process. The specimen was allegedly high purity zinc and the inference is that Superoxol produces pits at impurity free screw dislocations intersecting the basal plane.

Lines of pits were also observed which were interpreted as low angle twist or tilt boundaries. No mention is made of pit depths - no attempt was apparently made to measure pit parameters.

Straumanis and Wang (35) etched various faces of zinc with strong etchants such as HCl, H_2SO_4, $HClO_4$ and HNO_3. They found that the basal plane was attacked perpendicularly to a depth of 4-8 microns and then dissolution proceeded laterally. With the more concentrated acids, the pits became flat bottomed and resisted further attack while lateral attack proceeded. Often hexagonal pits are observed on the basal plane but according to Straumanis et al there is no reason to believe that such pits are associated with dislocations. They suggest that the dissolution

depends on the formation of a protective film as in the case of electropolishing. Small additions of aluminium magnesium and gold to the zinc crystals had no effect on the etch pit formation. Straumanis and Wang consider that pitting occurs followed by surface disintegration.

Rosenbaum and Saffren (23) studied the etching behaviour of the basal plane of high purity zinc monocrystals with a number of etchants. They found the most effective etchants to be halogens or halogen acids dissolved in ethyl alcohol. They preferred 90% ethyl alcohol, since with the suitable halogen acid concentrations the solution produced hexagonal pits, whereas the 100% based etchant tended to produce conical pits. Of the considerable number of etchants used, the two on which they reported most fully were 0.2-0.6M HCl and 0.2-0.6M HBr dissolved in 90% ethyl alcohol. The HCl etch produced pits with edges of the hexagons parallel to $<10\bar{1}0>$ while the HBr etch produced pits with edges parallel to $<11\bar{2}0>$. The authors considered that the pits formed were at the sites of emergent non-basal dislocations and that prior decoration is not required to produce pits, at least on the screw dislocations from the prism plane these dislocations being revealed directly after cleavage at liquid nitrogen temperatures. The edge dislocations from the pyramidal planes were introduced by deformation at 300°C (36) and so it is impossible to say whether decoration was effected in this case.

After deformation good if not exact correspondence was obtained on matched cleavage faces. Specimens were etched deformed and re-etched and flat bottomed pits were present at the sites of the original

pits and new sharp bottomed pits were present at new position of the dislocation. After deformation and under low magnification the pits, appearing as dots, were aligned in definite directions and in bending tests near the neutral axis the pit density was much reduced. Subsequent annealing caused a redistribution of pits. Many of the pits were arranged in rows which were considered to be sub-boundaries caused by polygonisation.

Thus there seems to be little doubt that Rosenbaum and Saffren were able to obtain good correlation between etch pits and emergent dislocations on the basal plane. They did not, however, claim to have revealed all the dislocations or that all the pits were at dislocation sites. They did, however, mention that the pits obtained were shallow and no attempt was made to estimate the depths of the pits. It is doubtful if an interferographic analysis of the surface would have shown the pits to be of measureable depth. Rosenbaum and Saffren, as do several other workers, claim to have used high purity zinc for their dissolution experiments. However, Regel et al have shown how sensitive to trace impurities is the etch pitting behaviour of metals and it must be borne in mind that small changes in metal purity or impurity content of the etchant may have significant results in the morphology of the etched surface.

Rosenbaum and Saffren (23) suggest that the reaction between zinc and HCl and HBr ethanolic etchants is oxidation of zinc by the hydrogen ion and by analogy with work by F. W. Young et al on electro-etching of copper, that the halogen ion acts as an inhibitor. Work by Young (37) has shown that bromine ion in solution slows the dissolution

FIGURE C

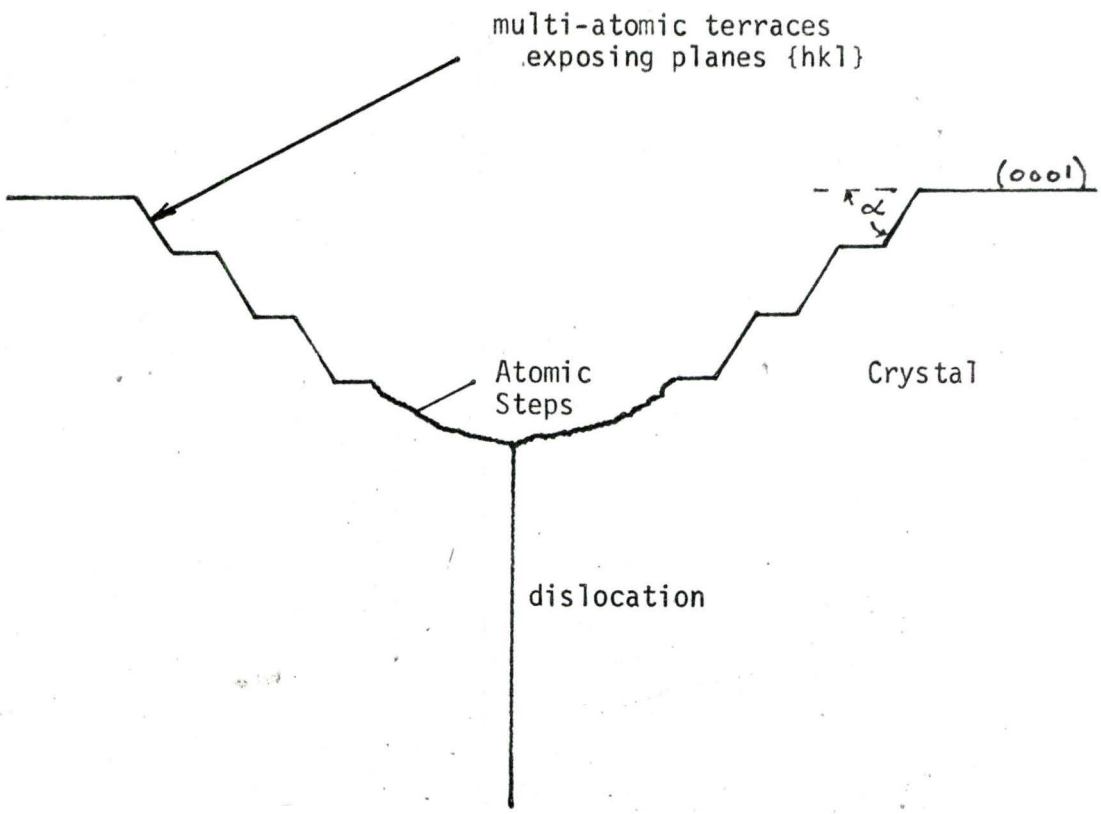
multi-atomic terraces
exposing planes {hkl}
(0001)
α
Atomic
Steps
Crystal
dislocation

rate of copper and extrapolation of this to zinc dissolution seems plausible both copper and zinc being of similar atomic size.

Rosenbaum and Saffren (23) analysed the gas evolved during the reaction by mass spectroscopy and found it to be hydrogen.

Whether or not the halogen ions act like an inhibitor like Fe^{+++} in LiF etching or how effective an inhibitor they are is not certain, but they do play a role in the dissolution of zinc. As previously mentioned chloride ions and bromide ion produce hexagonal pits on the basal plane of zinc, whose sides lie parallel to different directions, i.e. bromide ion retards ledges parallel to $<11\bar{2}0>$ most effectively while the chloride ion retards those parallel to $<10\bar{1}0>$ most effectively.

Rosenbaum and Saffren cite the work of Batterman (38) Irving (39) and Riessler (40) on prediction of pit slope. Riessler's geometric approach suggests that the pit will be bounded by crystallographic planes for which $\frac{W\alpha}{\cos \alpha}$ is smallest but greater than W(o) (fig.C). W(o) is the dissolution rate normal to the ground plane, in this case normal to the basal plane of zinc, the dissolution of the plane being unaffected by the dislocation. $W(\alpha)$ is the dissolution rate normal to the plane making an angle α with the basal plane. It is implicitly assumed that α is the overall angle of the pit facet. Since etching rates normal to the plane making an angle α with the basal plane are as yet unknown, Riessler's theory cannot be quantitatively verified.

Rosenbaum and Saffren found, as did Livingstone (41) on copper etching, pits with similar widths but different depths. This is not consistent with Riessler's analysis but agrees with the step motion

theory.

Livingstone (41) on his work on copper states that since pits have different depths and are all very shallow, multiatomic terraces are formed as opposed to monatomic steps. Rosenbaum and Saffren say that the pits formed on zinc may be made up of monatomic steps or multiatomic ledges, the latter being more likely by comparison with similar work on copper.

Chapter III

Experimental Techniques

(i) Growth of Single Crystals of Zinc

The crystal growing apparatus is shown in figure (D).

The technique employs a small furnace moving vertically upwards over a static polycrystalline zinc rod. The furnace was designed to have a temperature gradient with maximum temperature around 500°C. The furnace was driven by a small electric motor which was geared to raise the furnace at a constant speed. The electrical input is arranged such that a single switch starts the motor to raise the furnace and supplies current to the furnace heating element. The input power is cut off, when the furnace has traversed the zinc rod, by an electrical contact mounted in the furnace striking another contact on the apparatus.

The polycrystalline zinc rod is placed in a graphite tube which was drilled and reamed from a graphite rod to the required diameter.

Originally a freshly cleaved single crystal zinc seed was placed in the lower end of the graphite tube and molten zinc then cast on top, into the graphite tube. A better method was devised where the 99.999% pure zinc rod was machined to just fit the graphite mould.

The base of the graphite crucible sat on a brass water cooled stool through which cold water circulated at a constant rate. This was achieved by running the water through the stool via a constant head reservoir.

A pyrex tube enclosed the graphite mould and passed over two rubber seals on the brass stool. The top of the pyrex tube was

sealed with a rubber stopper in which was fitted a stopcock.

The brass stool was designed such that the pyrex tube could be evacuated using a 1/4 H.P. rotary vacuum pump, displacement 1.6 ft.^{3}/min. The evacuating tube was fitted with a two-way stopcock, one arm leading to the vacuum pump, the other to a cylinder to nitrogen.

(ii) Operation of Monocrystal Growing Apparatus

The graphite mould containing the zinc seed and poly-crystalline rod was seated on the brass stool. The pyrex tube was fitted over the stool and the stopcock at the top closed.

The cooling water was turned on and allowed to circulate through the stool.

The system was evacuated, flushed with nitrogen, re-evacuated and nitrogen slowly passed through the system and vented through the stopcock at the top of the pyrex tube to atmosphere via a water trap.

The furnace was wound down to an experimentally determined height and the power switched on, causing the furnace to rise at a constant rate of 7.5 cms./hr. and be raised to temperature.

The furnace travelled up the length of the graphite mould and the electrical input was automatically switched off when the furnace reached the required height.

After cooling, the pyrex tube was removed, and the zinc crystal knocked out of the graphite mould.

The crystal was cooled to liquid nitrogen temperature and cleaved by striking a sharp razor blade placed against the crystal. If the cleavage was normal to the axis of the rod, the crystal was placed

FIGURE D
Zinc Single Crystal
Growing Apparatus

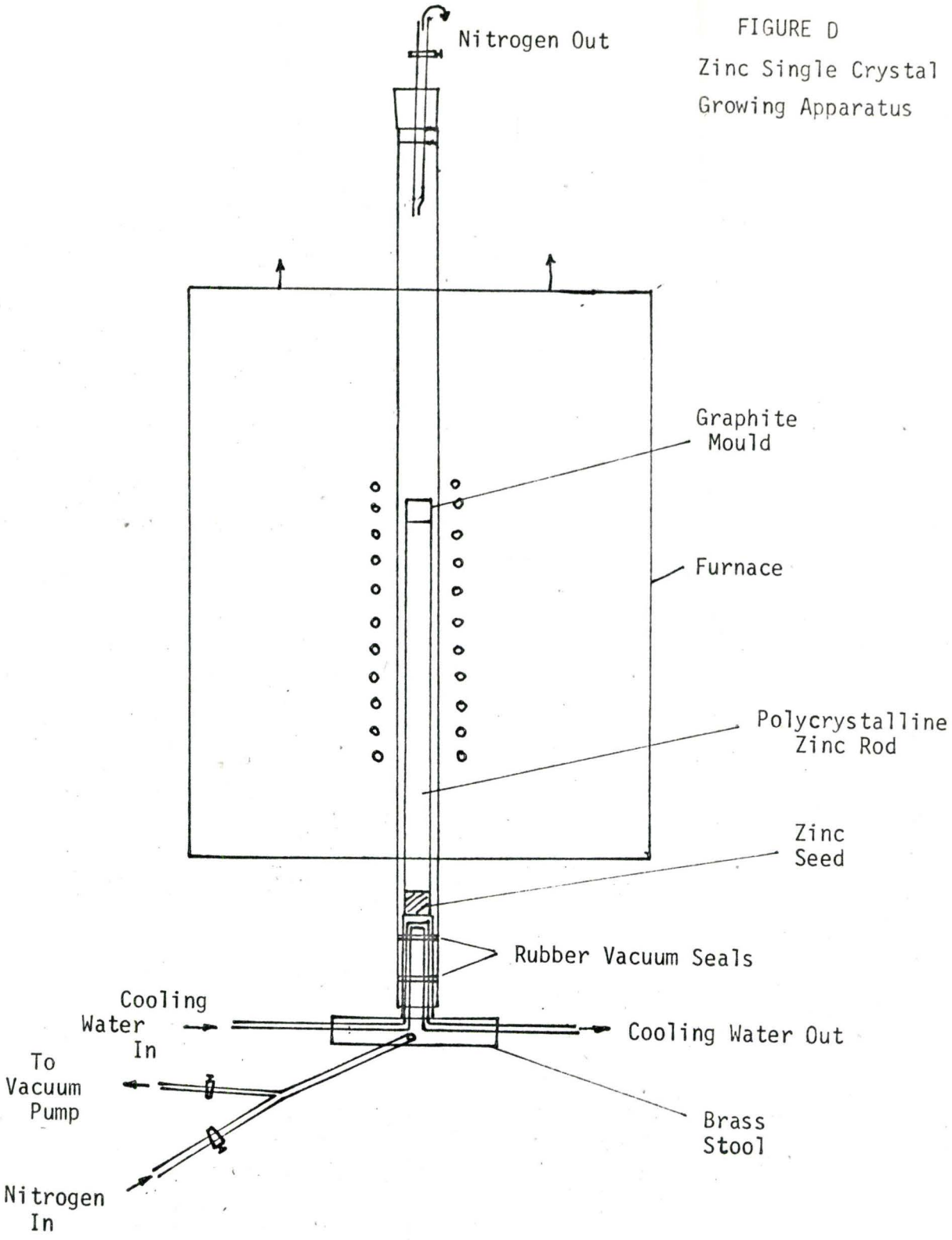

in ethanol which was raised to room temperature, then washed in ether, dried in a stream of air and carefully stored in a desiccator.

(iii) Specimen Preparation

A monocrystal rod of zinc was cooled in liquid nitrogen in a thermos and approximately 1/4" cleaved off the end using a sharp single-edged razor blade, a light hammer. The 1/4" long sample was quickly placed in ethanol and the ethanol temperature raised to 35°C. The specimen was then rinsed in ether and dried in a stream of air and placed in numbered plastic box prior to etching. Specimens were etched as quickly as possible after cleaving.

Specimens of length less than 1/4" tended to buckle upon cleavage, making it difficult to obtain useful interferograms.

On occasion, several specimens were cleaved at the same time. After each specimen was cleaved and placed in the ethanol bath, the bulk single crystal was returned to the thermos of liquid nitrogen before another specimen was cleaved. After drying, the specimens, in their plastic boxes, were placed in the desiccator.

(iv) Preparation of Etchants

The majority of the etching was done with a solution of HCl in 95% ethyl alcohol. The concentration range of HCl ranged from 0.03 MHCl to 2.4 MHCl. This is the etchant used by Rosenbaum and Saffren (23) except that more dilute and more concentrated solutions were employed. 95% ethyl alcohol was used as solvent as recommended by Rosenbaum and Saffren.

A few etching experiments were carried out using solutions

FIGURE E

Etching Apparatus

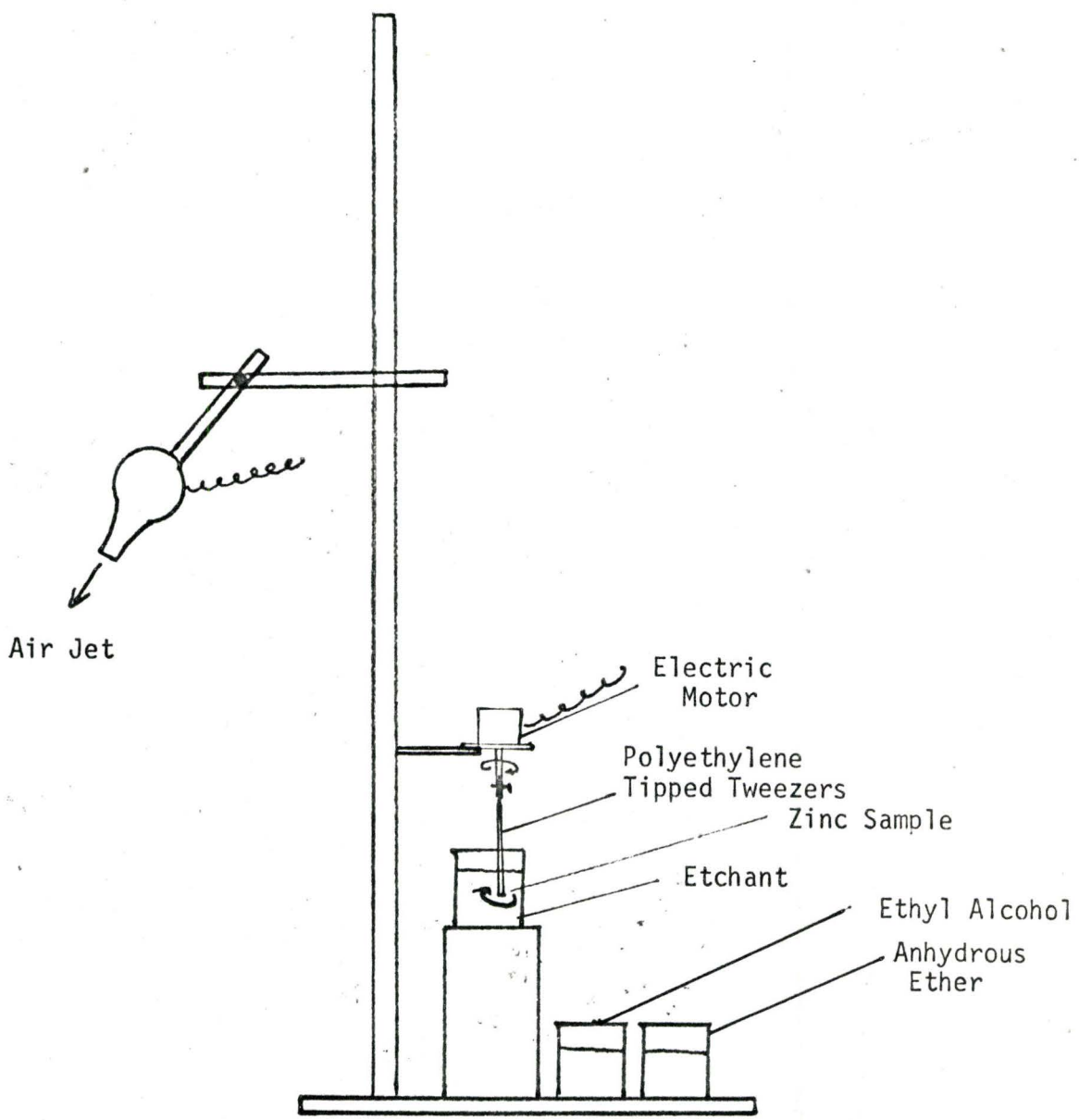

of HBr in 95% ethyl alcohol. These experiments were limited to the etchant concentration 0.24 MHBr and the experiments involved repeated etching on the same pits at successively longer times.

All the etchants used were prepared from a standard solution of 2.4 MHCl and 2.4 MHBr in 95% ethyl alcohol and the more dilute etchants obtained by addition of 95% ethyl to a fixed amount of the standard solution.

The standard solution was stored in a tightly stoppered polyethylene bottle and the solution was gently agitated before preparing the more dilute solution.

All etchants were prepared from a standard solution in an attempt to maintain uniformity of concentration of diluted etchants.

The etchants used were 0.03M, 0.06M, 0.12M, 0.3M, 0.6M, 1.2M and 2.4M HCℓ in 95% ethyl alcohol.

(v) Etching Techniques

The etching apparatus is shown in figure (E).

A small motor was designed to rotate a pair of polyethylene tipped tweezers, in which were gripped the specimens to be etched. The tweezers were attached to the shaft by means of a clamping screw, such that the specimens described a horizontal circle in the etching solution. The cleavage surface to be examined was the upper face of the specimen in the etchant. The etchant in a 50 ml. beaker was placed in position under the rotating specimen and the specimen etched for a fixed time. The rotating specimen was then washed in a beaker of 95% ethyl alcohol for approximately twenty seconds and then in anhydrous ether for ten

seconds and quickly dried in a stream of air. The dried specimens were carefully placed in the numbered plastic boxes, and examined microscopically on the interference microscope.

(vi) Examination of Etched Specimens

A Zeiss Interference microscope was used for the examination of the etched specimen. The specimen surface was examined under the lowest magnification and the most suitable areas were then located under maximum magnification, and the microscope switched to green light interference conditions with a wavelength of 0.54 microns. The interference patterns of the pits were then photographed using Kodak Plus-X 35 mm. film, with exposure time ranging from one to four minutes. This procedure was repeated for each specimen throughout the range of etchants and etch times used.

A photograph of a stage micrometer graduated in 1/100 mm. was taken with x10, x25, and x60 objectives to enable exact magnifications to be determined after photographic enlargements were made.

The Kodak Plus-X film was developed in Kodak Microdol diluted 1:3.

(vii) Repeated Etching Experiments

Several specimens were etched for short times and examined for promising pits and these regions of the surface photographed at maximum magnification on the Zeiss Interference microscope. The same specimen was then etched again for another fixed time and the same areas photographed. This procedure was repeated until the pits ceased to deepen and a photographic record of the deepening of various pits at

increasing etching times was obtained. This procedure was repeated for several regions on the surface of several specimens for a few etchants.

(viii) Etching Opposite Cleavage Faces

Some specimens were cleaved as previously described and the opposite faces of the cleavage were etched in the same etchant. Various corresponding regions of the opposite faces were photographed and compared.

(ix) Photograph Enlarging

The enlarger was set at a standard height for every negative. This was achieved by making an enlargement of the stage micrometer negative and for each batch of enlargements the enlarger was adjusted in height so that the image from the stage micrometer negative matched the standard photograph which was set in the masking plate. Thus the photographic enlargements all have the same magnification.

All the interferograms were printed on extra hard paper, developed in Vivadol followed by stop bath rinse, thorough fixing, washing and drying.

(x) Analysis of Photographs (Interferograms)

In most cases the interference fringes for pits took the form of concentric hexagons. To determine the profile of the pits the following procedure was adopted. A sheet of cm./cm. graph paper was trimmed on three sides.

The graph paper was then laid across the photograph of the

DIAGRAM I

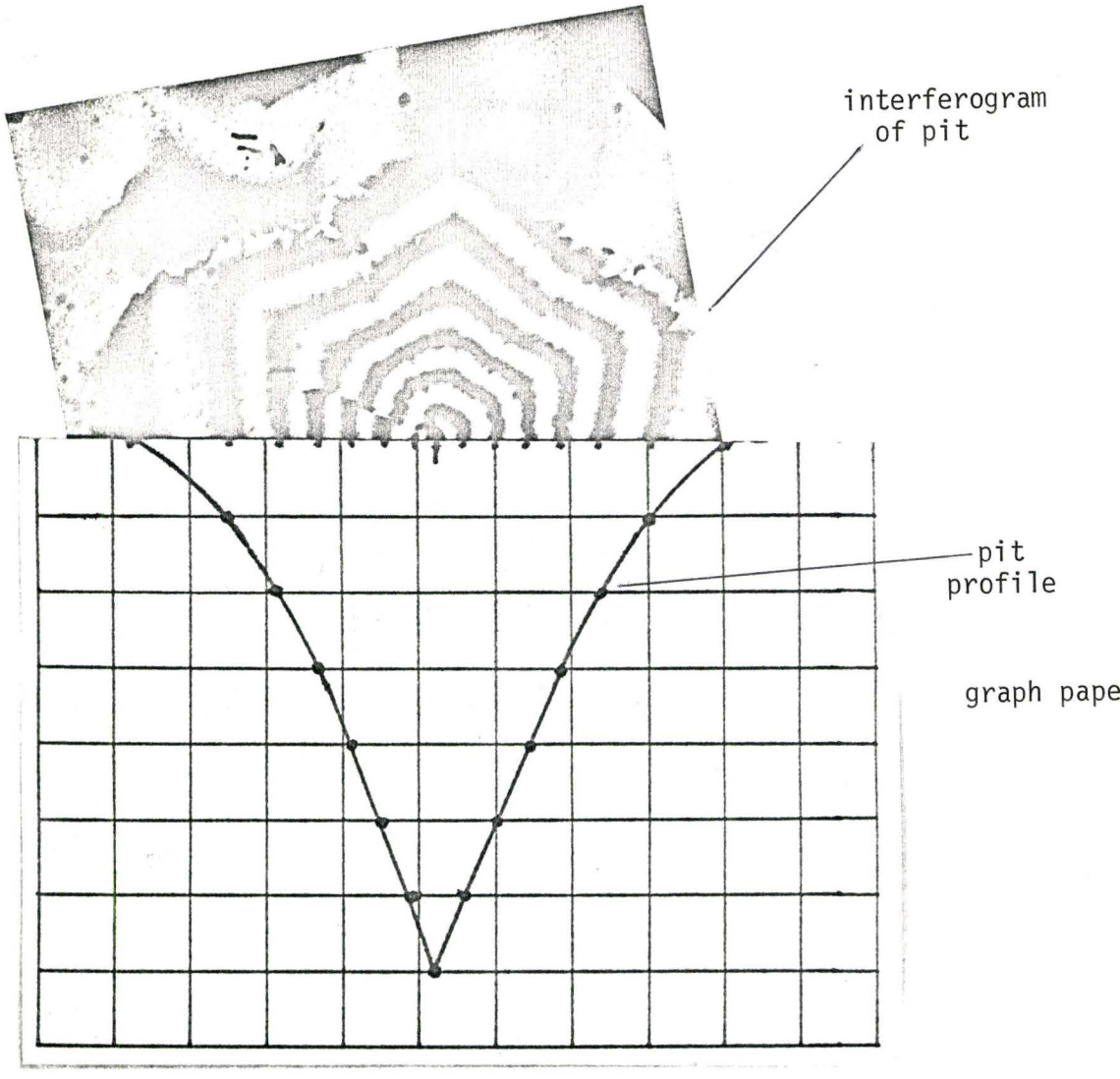

pit cutting the centre of opposite sides of the hexagon and the pit centre. At each point on the graph paper where a fringe intersected the graph paper a point was marked on the graph paper - the centre of fringes were used. The point on the graph paper corresponding to the fringe furthest from the centre of the pit became the datum of surface of the sample. The next point was marked one centimetre below the point on the edge of the graph paper and so on till the centre of the pit was reached where the points were elevated one centimetre per fringe from the pit centre to outside of the pit. The points were joined and the trace revealed the pit profile. Generally the points near to the pit centre were collinear and this was the measured slope. As the outside of the pit was approached the fringes became further apart and the pit slope decreased. Thus the pit slope was generally convex. The analysis is represented on diagram (I).

A table was drawn up for each etchant, for each etch time and the pit number recorded. Opposite the pit number was marked the angle of both sides of the profile as measured by protractor, and the pit depth in centimetres. The profile angles were converted to the true tangent.

By calculating the magnification of the photograph, using the photograph of the stage micrometer and knowing the distance between two fringes, 0.27 microns, it was possible to calculate a factor to convert the tangent of the protractor measured pit profile angle to the true tangent of actual pit angle and hence the true angle of the pit. The protractor measured angle and tangent were designated θ and tan θ and the actual angle and actual true tangent, θ' and tan θ' respectively.

The rate of deepening d/t, was calculated

t ≡ etching time in seconds

d ≡ pit depth

for each etching time in each etchant for each pit and the parameter $d/t / \tan \theta' = K'$ calculated.

The mean value of K' for each etching time in each etchant was calculated and the standard deviation evaluated.

The values of K', θ', and d/t were tabulated for the complete range of etchants and etch times. In addition each system - particular etchant at a fixed time - was examined to check for pits with anomalous results and to check whether pits with different slopes and depths within the same system produced a constant value of K'.

Graphs were drawn of pits depths against etching time at constant etchant concentration for the series of experiments where repeated etching of the same sample was done for increasing etching times.

A histogram of true pit angle was constructed to determine the slope distribution.

Chapter IV

Results

i) Introduction

ii) Successive etching experiments using HCl and HBr dissolved in 95% ethyl alcohol

iii) Results of zinc etching over a range of etchant compositions (HCl in 95% ethyl alcohol over a range of etching times

iv) Etching experiments on deformed specimens

v) Etching experiments on matching cleavage faces

(i) Introduction

Successive etching of the same pits on various specimens in an etchant concentration range suggested by Rosenbaum and Saffren (23) were performed in order to ascertain that the initially nucleated pit was the site of a linear defect.

Etching experiments were then carried out over a wide range of etchant concentrations, beyond the limits suggested by Rosenbaum and Saffren and for a range of times at each etchant composition. A considerable number of pits were analysed for each etchant "condition" (particular etchant concentration at a fixed time). A considerable spread of parameters occurred and a histogram of pit slopes was constructed and on this basis the data was summarised in the form of three tables corresponding to slopes around 5°, 2 1/2° and 1 1/2°. The bulk of the pits examined had slopes around 5° and these pits correspond to the pits which were examined in the successive etching experiments.

In attempts to determine which defects caused the different pits, some specimens were deformed by various techniques prior to etching and attempts were made to obtain matching cleavages.

(ii) Successive Etching Experiments

Successive etching experiments were performed on several specimens at four HCl etchant compositions, 0.12M, 0.24M, 0.30M and 0.5M HCl and at 0.24M HBr. Only the deeper pits corresponding to those on table I were examined.

With the HCl etchant an optimum time was reached with each etchant beyond which the original pits ceased to deepen and in fact

appear to become shallower due to general surface attack. The series of experiments using 0.24M HBr in 95% ethyl alcohol produced much deeper pits and a slower rate of attack. Etching times more than three times as long producing deepening pits as compared with the same concentration of HCl.

The pits produced by the HBr etchant were largely non-crystallographic and tended to be almost conical.

The results of these experiments with the different etchant compositions, where the individual pits were followed for increasing etching times are summarised in the depth against time graphs figures (13 to 17) and by interferograms (1a-g to 2a-f).

(iii) Results of Etching over Range of HCl Concentrations and Times

Cleaved monocrystal discs were etched in solutions of HCl in 95% ethyl alcohol for times from 10 seconds to 240 seconds and etchant concentrations from 0.03M HCl to 2.4M HCl.

From the pit profiles obtained from the interferograms values of the actual angles (θ') made by the pit sides to the (0001) cleavage plane were calculated and the depth (d) measured. Thus values of tan θ' and rate of deepening were found and $K' = \frac{d/t}{\tan \theta'}$ calculated. The mean value of K' was found for each etchant "condition" (constant etchant concentration at fixed time) and the mean deviation calculated.

Table I shows a summary of the assembled data, giving for each "etchant system" the mean value of K', θ' and d/t. θ' is measured in degrees and d/t in microns/second.

The mean deviations for K' are not included but it was

generally found to be about $\pm$ 10%.

At low etchant concentrations measurable pits only appeared after longer etching times and with increasing etchant concentration an optimum etching time was reached for each etchant beyond which the pits ceased to deepen, which explains the absence of data at longer etching times for the more concentrated etchants.

Figures (18 and 19) show a sample of the interferograms corresponding to the conditions of table I.

Table I and figures (18 and 19) summarise the data for the majority of the measured pits. However a considerable number of pits differ appearance from those depicted in figures (18 and 19). These pits are less deep and have a lower pit side slope than the pits shown on table I under identical etching conditions on the same cleavage face. Examination of these pits showed that they fell into two groups having pit slopes around 2.5° and 1.5°. Tables II and III were constructed similar to table I for these two groups of pits and figures (2 to 11) show examples of interferograms of these pits.

Table I which summarises the bulk of the data collected shows definite trends in parameters. An important observation is that the value of K' is not constant either for constant etching time or at different etching times with the same etchant. There is however a trend in the values of K' for a constant etching time with increasing HCl concentration the value of K' increasing. At constant HCl concentration and increasing etching time K' decreases.

The angles the pits make with the cleavage plane are fairly

constant. The histogram figure (20)) shows that a definite peak occurs between 4.5° and 5.5° i.e. the order of pit slope occurring in table I. There are however some "etchant conditions" where this mean angle is exceeded. The angles of pits etched in 0.03M HCl have a much higher slope and also a considerable scatter in values. There is also a tendency at the various etchant concentrations for slopes of the pits at the lower etching times to have higher slopes, suggesting that initially the pit slope is higher and is reduced slightly with increasing etching time.

In a number of etchant systems e.g. 60 seconds at 0.06M HCl different values of K' are obtained. The rate of deepening of the two pit types is fairly constant but the pit slope variation causes a vastly different value of K'.

The 10 second etch at 1.2M HCl also produces two K' values, one twice the value of the other. In this case the pits with the lower rates of deepening have higher pit slopes. However, this series of pits has a wide range of depths and slopes, from 5° to 9.5° the deeper pits having the steeper sides giving a $\pm$ 5% mean deviation on the value of K'. The steeper series of pits (1.2M HCl for 10 seconds) are distinctly anomalous and it is possible that the etching apparatus was contaminated possibly with a trace of $AgNO_3$, in apparatus which was concurrently but independently being employed for different dissolution experiments.

In most etchant systems there is some spread of depths and slopes but generally steeper pits are deeper and a constant value of K' is obtained within experimental error.

The etchant "condition" 0.12M HCl at 120 seconds etching produces a constant K', value 0.116 $\pm$ 10% from two series of pits with mean slopes of 7.2° and 5.0° and mean rates of deepening of 0.015 microns/second and 0.010 microns/seconds respectively.

Some pits in a particular etchant system have similar slopes to the majority of the pits but have smaller depths. These shallower pits are most probably due to defects which did not intersect the cleavage face prior to etching but were revealed at some time = t' seconds due to general surface attack. Thus since t' is unknown the rate of deepening cannot be computed and the data from these pits is ignored in calculating a mean value of K'.

There is also a tendency for pits to become flat or round bottomed. For pits which have just begun to become round bottomed and which are of sufficient depth, extrapolated values of depth may be used to obtain d/t and K'. However, drastic extrapolations must be excluded as pits generally become less steep (diag. I) as distance from the source increases and large extrapolations would lead to an underestimation of both pit slopes and depths. Such pits are excluded from the data when K' is computed.

Tables II and III show the same general trend in K' values as table I with the smallest value of K' occurring with the dilute etchant at long etching times and largest value of K' occurring for the shortest etching time in the most concentrated etchant. Table II is compiled for pits with slopes around 2.5° and table III for pit slopes around 1.5°

While the trend of K' values for tables II and III are similar to table I there are some different features. For the same etchant system the K' values for table II pits are similar to table III pits despite different d/t and θ' parameters.

For the three times at 0.06M HCl the value of K' is fairly constant including both tables II and III.

For etchant systems 120 seconds at 0.6M HCl and 0.3M HCl six different mean slopes, from 1.5° to 3.3° with different d/t values give a constant value of K'. The constancy in K' is not maintained at these concentrations at longer or shorter etch times.

(iv) Etching Deformed Specimens

Figures (21 and 22) show micrographs of specimens which were intentionally deformed. Various methods were tried to produce dislocations which intersected the basal plane. Some specimens were scratched on the outside prior to cleavage. The specimen was then cleaved normal to the scratch thus producing a notch on the sample perimeter which acted as an aid to location of the area of local deformation. After etching the area adjacent to the notch showed dark closely spaced parallel bands in which the individual pits (observed) as small dots were just visible. It is considered that these pits are the sites of emergent dislocations on the basal plane. However, the pits were very much smaller than the pits which were investigated by interference microscopy. Thus the pits produced by scratching the specimen did not correspond to the pits corresponding to the data on Tables I, II and III.

A monocrystal rod about 1" in length was held at 350°C for

one hour and then rapidly removed from the furnace deformed by compression normal to the basal plane in an attempt to introduce screw dislocations on the prism planes of the zinc monocrystal. Great difficulty was encountered in cleaving this deformed rod even at liquid nitrogen temperature and in fact no good cleavage surfaces were obtained. Due to the uneven cleavage it was difficult to focus the interference microscope on the etched surface and obtain interferograms. However, though there appeared to be an increase in the number of small pits, not measurable by interference techniques, the number of large pits did not appear to be affected by the high temperature deformation.

(v) Matching Cleavage Faces

Attempts were made to match opposite cleavage faces but little success was achieved.

A specimen which was annealed for one hour at 350°C and etched did not show any noticeable increase in the number of deep pits formed.

Chapter V

Discussion of Results

The main purpose of this project was to examine the relationship between the rates of etch pit deepening and the slopes of the etch pits formed on the basal plane of zinc monocrystals over a range of etching times and HCl solutions in 95% ethyl alcohol for a range of HCl compositions.

The ratio $d_{pit}/t/\tan\theta'$ was designated by K'. Before discussing the results of the investigation this concept will be briefly reviewed.

$$K = \frac{d_{(defect)}}{t} / \tan\theta'$$

$$= \frac{d_{(s)} + d_{(pit)}}{t.\ \tan\theta'}$$

d_s = depth of general surface attack.

It is assumed that $d_s/t = V_s \equiv$ rate of attack of (0001) plane is constant.

$$\therefore K' = \frac{d_{(pit)}/t}{\tan\theta'}$$

The results of measurement on etch pits are summarised on Tables I, II and III.

Considering Table I, which comprises the bulk of the data and the steepest sided and deepest pits, it is observed, as expected, that at constant etching times the rate of pit deepening - $\frac{d_{(pit)}}{t}$ - increases with increasing etchant concentration due to increased chemical attack. However, the value of the pit slope does not vary greatly or in

any systematic fashion with increasing etchant concentration and so K' is approximately proportional to $\frac{d_{pit}}{t}$, and so K' increases with increasing etchant concentration at constant etching times.

At fixed etchant concentration and increasing etching time K' decreases with increasing etching time. Again tan θ' is fairly constant for each etchant and so again K' is approximately proportional to d_{pit}/t. The experiments performed, successively etching the same pit for increasing times, shows that the pit depth does not increase linearly with etching time and this explains the decreasing value of $d_{(pit)}/t$ and hence of K'.

Generally Tables II and III follow the same pattern as Table I.

Physically K' represents the velocity of ledges away from the source i.e. V_L or $\frac{\text{width of pit}}{2.t.}$, the rate of pit widening and at constant t, 2K't is the pit width measured in the region of the pit where the pit slope is constant. Thus for example at constant etching time, for the pits of Table I, increasing etchant concentration produces pit profiles which are successively deeper and wider but with essentially the same slope. It is assumed that the pits of Table I are produced by attack of the same defect and since the slope is unchanged with increasing chloride ion concentration, then it must be concluded that the chloride ion has no inhibiting effect on ledge motion away from the source, since chloride ion acting as a ledge poison should increase pit slope. Thus the slope and rate of widening of the etch pit must be controlled by the rate of nucleation at the defect source. With increasing etching times at constant etchant concentration the decrease

in the rate of pit widening must be due to the decrease in the rate of pit deepening as etching times increase.

Tables II and III have lower pit slopes, Table II mean slope being about 2.5°, Table III about 1.5°. Presumably these pits are the result of attack at different defects. However, the K' values of pits for the same etchant "conditions" in Tables II and III are substantially the same. Thus different defects, though they have different rates of deepening, under constant etching conditions, i.e. constant concentration of HCl, have the same rate of widening and so the growth of the pit is dependent on the defect causing its formation rather than on the etchant. In many cases especially with etchant concentration from 0.06M to 0.6M HCl, Table I pits have similar values of K' as those of Tables II and III for the same etchant conditions. With the Table I pits the equality in K' values breaks down with the pits produced by 2.4M HCl and for the shorter etching times in 1.2M HCl. Thus for the bulk of the pits examined at constant etching "conditions" K' is a constant.

Generally the pits assume a hexagonal shape. It is found that with pits from Table I that the fringes closest to the pit centre tend to be circular, becoming hexagonal further from the centre and sometimes becoming extremely ragged near the surface. It is probable that the effect of HCl, apart from its property as the oxidant, is to stabilise facets parallel to certain directions. Rosenbaum and Saffren suggest that HCl stabilised pit edges parallel to $\langle 10\bar{1}0 \rangle$ directions. However, it is observed that the six sides of the hexagons are not quite straight, but that each side forms a shallow Vee pointing towards the

pit centre. This suggests that the HCl stabilises twelve facets with directions slightly misorientated from the <10$\bar{1}$0> directions. At the periphery of the pit the raggedness of the fringes is probably due to the outward moving ledges interfering with the features produced by general surface attack. At the pit centre the conical shape of the fringes may be due to insufficient time being available for the faster growing facets to be eliminated and the slower growing facets producing the hexagonal - or near hexagonal - shape have not yet become dominant. It is found that with the very dilute etchants that the conical nature of the pit is more persistent suggesting that with the low HCl concentrations and lower rate of attack the faster growing facets are less rapidly eliminated and the hexagonal symmetry more slowly attained. Thus it is proposed that the HCl function in the etching experiments is to act as the oxidant and to stabilise directions parallel to <10$\bar{1}$0>.

The few experiments done with HBr in 95% ethyl alcohol as the etchant produced deeper pits and a slower rate of attack than the same concentration of HCl. This result is similar to that found by Young (57) on copper etching and suggests that the bromide ion is acting as an inhibitor in the etching process. The pits formed by the HBr etchant are conical near the pit centre and then the fringes become scalloped further from the centre, suggesting that the circular ledges moving out from the pit source are being pinned - possibly by bromide ions or aggregations of bromide ions - causing the ledges to bow out between the pinning points. At the periphery of the pits formed by HBr there is an attempt to produce a hexagonal shape to the pits though this tends to be imperfectly formed. It is suggested that HBr etchants as

opposed to HCl etchants control the pit formation more through an inhibiting action than by crystallographic control.

The deformation experiments performed on the zinc specimens followed by etching with HCl solutions suggest that the pits analysed in this work were not "fresh" dislocations. Deformation normal to the basal plane at 300°C should introduce screw dislocations from the prism planes. These deformed samples were extremely difficult to cleave. Since the cleavage crack forms a step each time it intersects a screw dislocation (42), it is probable that the deformation process produced the required screw dislocations which cause a large increase in energy to be required to propagate the cleavage crack across the specimen. Thus the cleavages produced were poor but no increase in the density of the types of pits analysed and summarised in Tables I, II and III was found. Similarly, scratching the outside of the specimen produced closely packed lines of pits close to the scratch. These pits were attributed to dislocations intersecting the surface but they were very much smaller than the pits investigated during this work.

In hexagonal close packed metals (43), there are three types of dislocations which intersect the basal plane at 90°. Screw dislocations $\{10\bar{1}0\}\ \langle\bar{1}2\bar{1}0\rangle$, edge dislocation $\{0\bar{1}\bar{1}0\}\ \langle\bar{2}110\rangle$, mixed $\{0\bar{1}\bar{1}0\}\ \langle\bar{2}113\rangle$. It is possible that these dislocations could be responsible for the etch pits observed in this study and outlined in Tables I, II and III. However, the deformation studies indicate that "fresh" dislocations do not form deep pits and so it is postulated that the pits analysed in this work are impurity pinned dislocations. Rosenbaum et al mention the existence of isolated deep pits which were relatively immobile during

room temperature deformation and in the present work the density of deep pits was also low. What the impurities segregated at these dislocations are, is unknown since a considerable number of impurities - in small concentrations - are present in the zinc. It is not possible to say whether the three types of pits outlined in Tables I, II and III are the result of different dislocation types or due to different segregated impurities, assuming that the pits formed are at sites of emergent dislocations.

Chapter VI

Conclusions

1) K' - a measure of the rate of pit widening is largely constant for the same etchant conditions but different defect types. This suggests that the growth of the pit is dependent on the defect and not on the etchant.

2) (a) For the same defect K' increases with etchant concentration for fixed etching time since K' is approximately proportional to d_{pit}/t.

(b) For the same defect K' decreases with increasing etching time at constant etchant concentration due to decreasing rate of pit deepening with etching time.

3) The HCl/ethyl alcohol solution is considered to act as an oxidant $2H_{(s)}^{+} \rightarrow H2_{(g)}$ and to control the pit shape but to have no effect on inhibition like ferric ion in LiF etching.

4) The HBr/ethyl alcohol etchant produces a slower rate of attack, deeper pits and has less crystallographic control on pit shapes. It is possible that the bromide ion has an inhibiting effect on ledge motion.

5) Deformation experiments suggest that the HCl etchant does not produce dislocation etch pits measurable by interference microscope techniques and so the pits investigated were not due to "fresh" dislocations intersecting the basal plane.

6) It is suggested that the pits investigated in this work were the sites of impurity decorated dislocation intersecting the basal plane. Three possible dislocation types could be responsible.

Suggestions for Further Work

1) It would be of interest to investigate the pits formed by the HBr etchants over a range of etchant concentrations and etch times to see whether the bromide ion has an inhibiting effect on ledge motion and to compare the numerical results with HCl etchants of the same concentration.

2) An electron microscope study of the etching of the basal plane by HCl and HBr etchants dissolved in ethyl alcohol would give a physical picture of the ledge formation and may produce data on the effect of the anion on ledge motion and pit morphology.

3) Zinc crystals doped with different quantities and types of impurities should indicate whether impurity decorated dislocations cause the deep pits.

4) Use of different alcohols as solvents for HCl and HBr would indicate whether the alcohol plays any role in the formation of etch pits.

References

1. W. Kossel, Nachr. Ges. Wiss. Göttingen 135 (1927).
2. F. C. Frank in "Growth and Perfection of Crystals", John Wiley & Sons, New York 1958.
3. W. K. Burton, N. Cabrera, F. C. Frank, Phil. Trans. Roy. Soc. 243A, 299 (1951).
4. N. Cabrera, M. M. Levine, Phil. Mag. 1, 450 (1956).
5. J. P. Hirth, G. M. Pound, J. Chem. Phys. 26, 1216 (1957).
6. W. W. Mullins, J. P. Hirth, J. Phys. Chem. Solids 24, 1391 (1963).
7. F. C. Frank, M. B. Ives, J. App. Phys. 31, 1996 (1960).
8. M. B. Ives, J. App. Phys. 32, 1534 (1961).
9. J. J. Gilman, W. G. Johnston, G. W. Sears, J. App. Phys. 29, 747 (1958).
10. J. J. Gilman in "The Surface Chemistry of Metals and Semiconductors", Ed. H. C. Gatos, John Wiley & Sons, New York, 1959, p. 136.
11. N. Cabrera, ref. (10), p. 71.
12. W. G. Johnston in "Progress in Ceramic Science", Vol. 2, Pergammon Press, New York, 1962, p. 1.
13. M. B. Ives, J. P. Hirth, J. Chem. Phys. 33, 517 (1960).
14. J. J. Gilman, W. G. Johnston, J. App. Phys 29, 877 (1958).
15. T. R. Ramachandran, M. B. Ives, Tech. Rep. No. 6 to U. S. Office of Naval Research (Metallurgy Branch) Contract Nonr. 3925(00), June 1966.
16. M. B. Ives, M. Baskin, J. App. Phys. 36, 2057 (1965).
17. T. R. Ramachandran, M. B. Ives, Tech. Rep. No. 7 to U. S. Office of Naval Research (Metallurgy Branch) Contract Nonr. 3925(00), July 1966.
18. A. P. Honess, "Etch Figures on Crystals", John Wiley & Sons Inc., New York, 1927.

19. J. W. Faust Jr. as ref. (10), p. 152.

20. F. W. Young Jr., J. App. Phys. 33, 749 (1962).

F. W. Young Jr., J. App. Phys. 33, 963 (1962).

F. W. Young Jr., J. App. Phys. 33, 3553 (1962).

F. W. Young Jr., J. R. Savage, J. App. Phys. 35, 1917 (1964).

L. D. Hulett Jr., F. W. Young Jr., J. Phys. Chem. Solids 26, 1287 (1965).

F. W. Young Jr., L. D. Hulett Jr. in "Metal Surfaces" (Edited by W. D. Robertson and N. A. Gjostein) A.S.M., Metals Park Ohio (1963) p. 375.

21. D. A. Vermilyea, Acta. Met. 6, 381 (1958).

22. J. W. Faust Jr. as ref. (10), p. 156.

23. H. S. Rosenbaum, M. M. Saffren, J. App. Phys. 32, 1866 (1961).

24. J. W. Faust Jr. as ref. (10), p. 160.

25. J. J. Gilman et al as ref. (9).

A. G. Tweet, J. App. Phys. 30, 2002 (1959).

J. W. Faust, H. F. John, Bull. Am. Phys. Soc. 5, 165 (1960).

26. R. Steadman, J. D. Pugh, Phil. Mag. 12, 967 (1965).

27. R. L. Fleisher, R. M. Walker, Phil. Mag. 13, 1083 (1966).

28. A. H. A. Meleka, Phil. Mag. 1, 803 (1956).

29. V. R. Regel, V. M. Stepanova, Sov. Phys. 4, 204 (1959).

30. J. J. Gilman, Trans. A.I.M.E. 206, 998 (1956).

31. J. V. Sharp, Phys. Stat. Sol. 8, 1, K1. (1965).

32. J. J. Gilman, V. J. De Carlo, Trans. A.I.M.E. 206, 511 (1956).

33. R. C. Brandt, K. H. Adams, T. Vreeland Jr., J. App. Phys. 34, 587-590, 591-594 (1963).

34. J. George, Phil. Mag. 4, 1142 (1959).

35. M. E. Straumanis, Y. Wang, Tech. Rep. No. 13 to U. S. Office of Naval Research Contract Nonr. 2296(03), Oct. 1965, Corrosion 23, 132 (May 1966).

36. J. J. Gilman, Trans. A.I.M.E. 206, 1326 (1956).

37. F. W. Young Jr., J. App. Phys. 32, 192 (1961).

38. B. W. Batterman, J. App. Phys. 28, 1236 (1957).

39. B. A. Irving, J. App. Phys. 31, 109 (1960).

40. W. Riessler, Z. angew. Phys. 12, 433 (1960).

41. J. D. Livingstone in "Direct Observations of Imperfections in Crystals", Am. Inst. of Mining, New York 1962, Eng. Interscience.

42. J. J. Gilman, Trans. A.I.M.E. 212, 310 (1958).

43. A. W. Ruff, Ph.D. Thesis, University of Maryland, p. 116 (1964).

44. W. G. Johnston, J. J. Gilman, J. App. Phys. 30, 129, 1959.

45. L. D. Hulett Jr., F. W. Young Jr., J. Electrochem. Soc. 113, 410, (1966).

46. P. Lacombe, L. Beaujard, J. Inst. Metals 74, 1 (1948).

47. G. Wyon, P. Lacombe, "Report of Conference on Defects in Solids", Bristol 1955, p. 187.

48. V. E. Wolff, Acta Met. 6, 559 (1958).

49. R. W. Guard, Trans. A.I.M.E. 218, 573 (1960).

50. L. C. Lovell, F. L. Vogel, J. H. Wernick, Metal Progress 75, 96 (1959).

51. I. Berlec, J. App. Phys. 33, 197 (1962).

52. L. D. Dyer, J. Electrochem. Soc. 112, 624 (1965).

53. A. A. Bochvar, Yu P. Pschenichnov, Sov. Phys. (Dokl) 10, 491, (1966).

FIGURE 1 0.24 Molar H Br

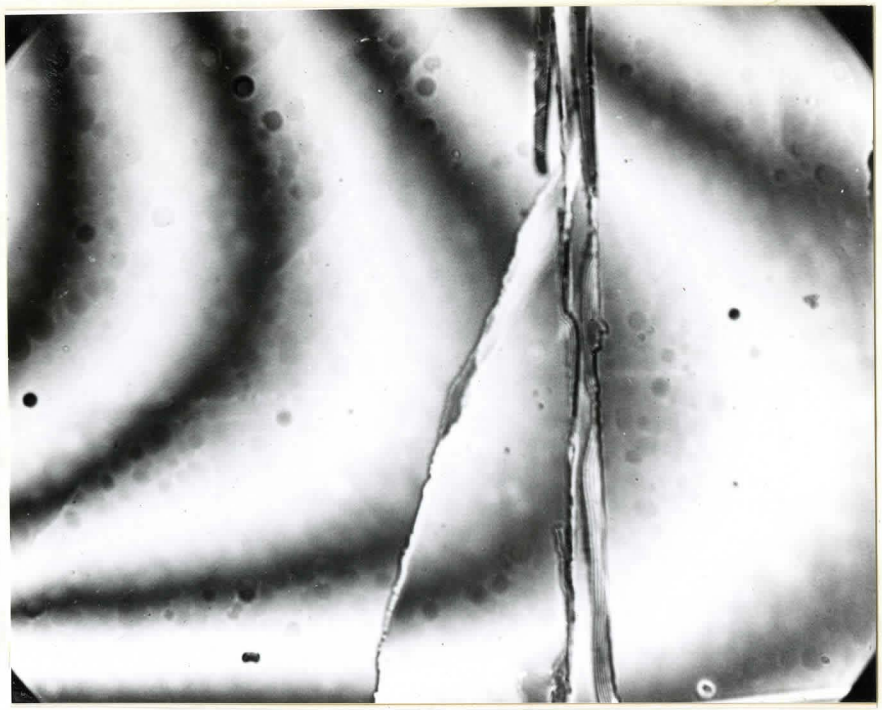

Fig. 1 (a) 10 sec. etch

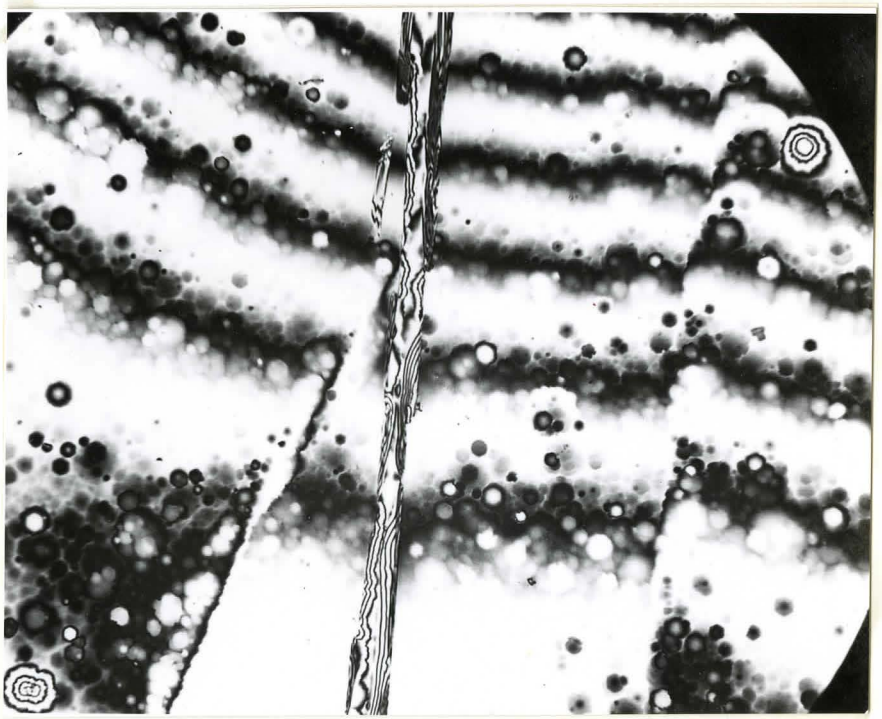

Fig. 1 (b) 60 sec. etch

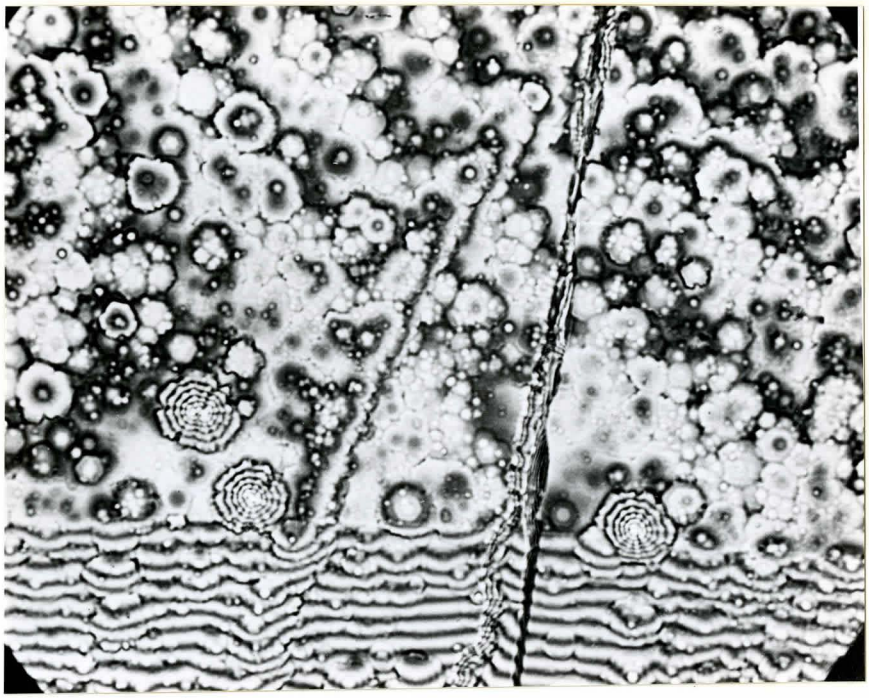

Fig. 1 (c) 180 sec. etch

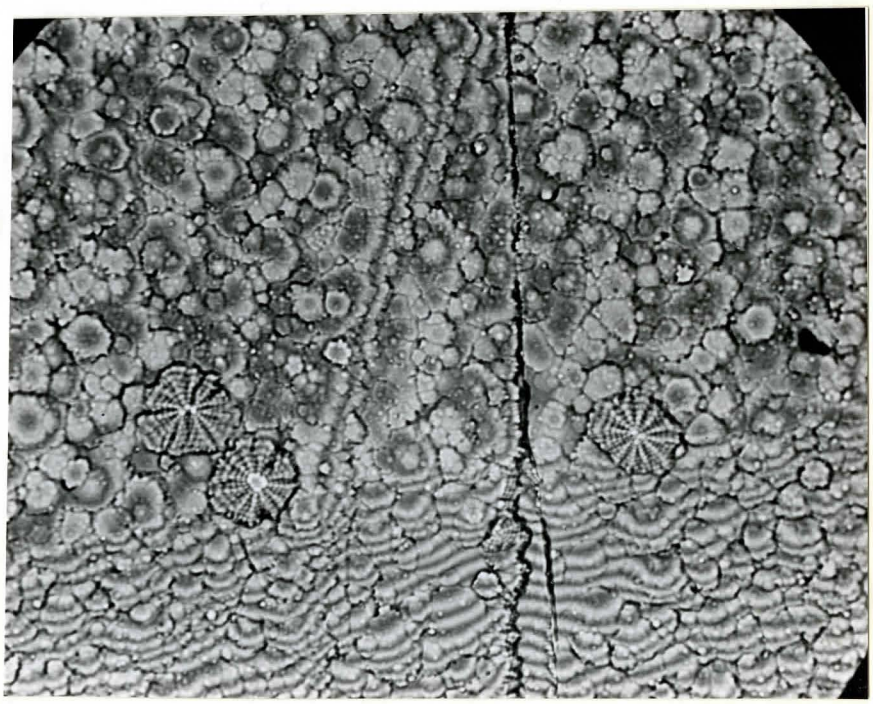

Fig. 1 (d) 300 sec. etch

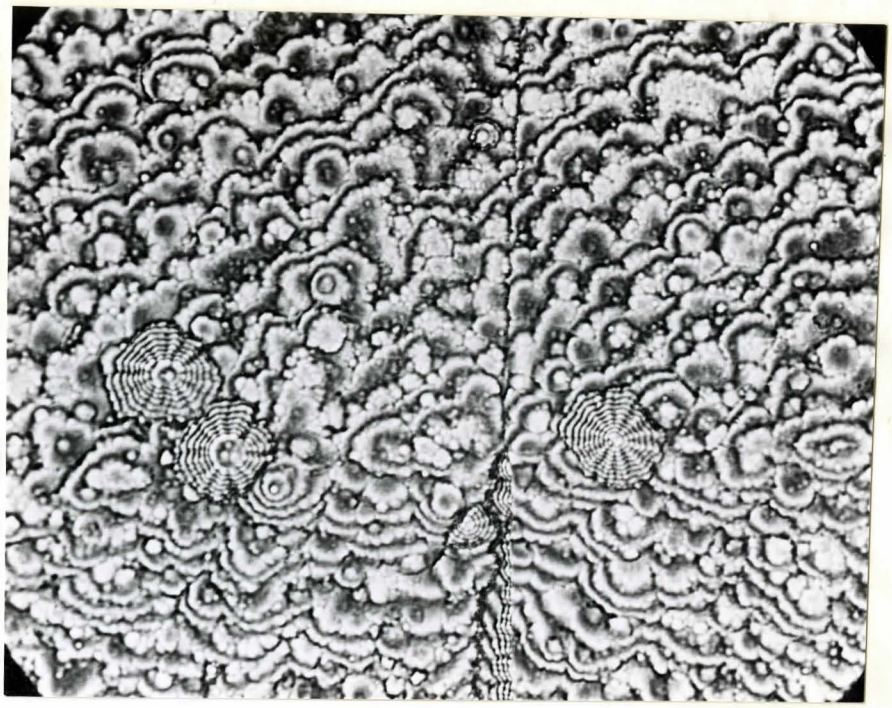

Fig. 1 (e) 420 sec. etch

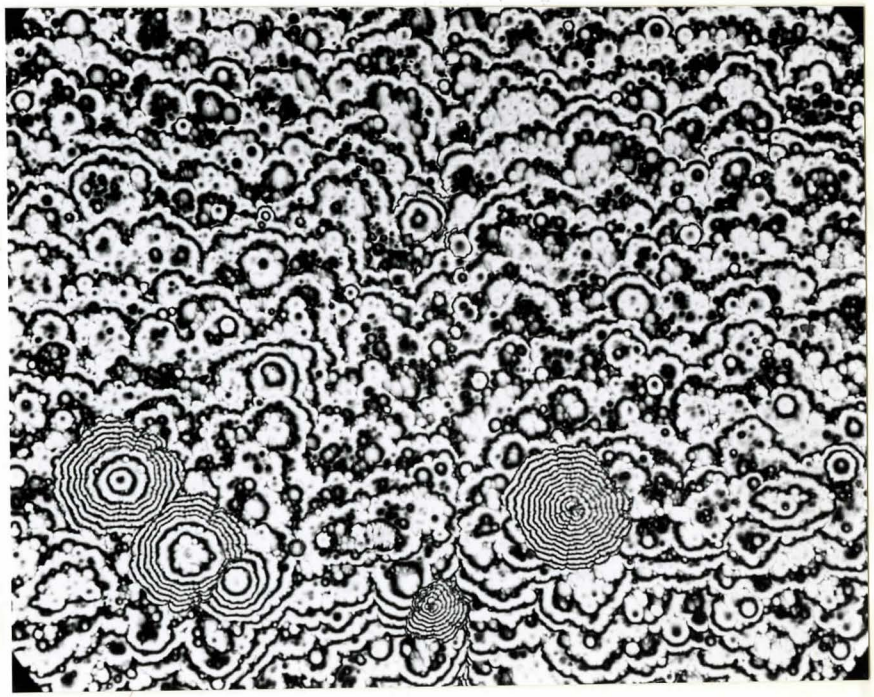

Fig. 1 (f) 600 sec. etch

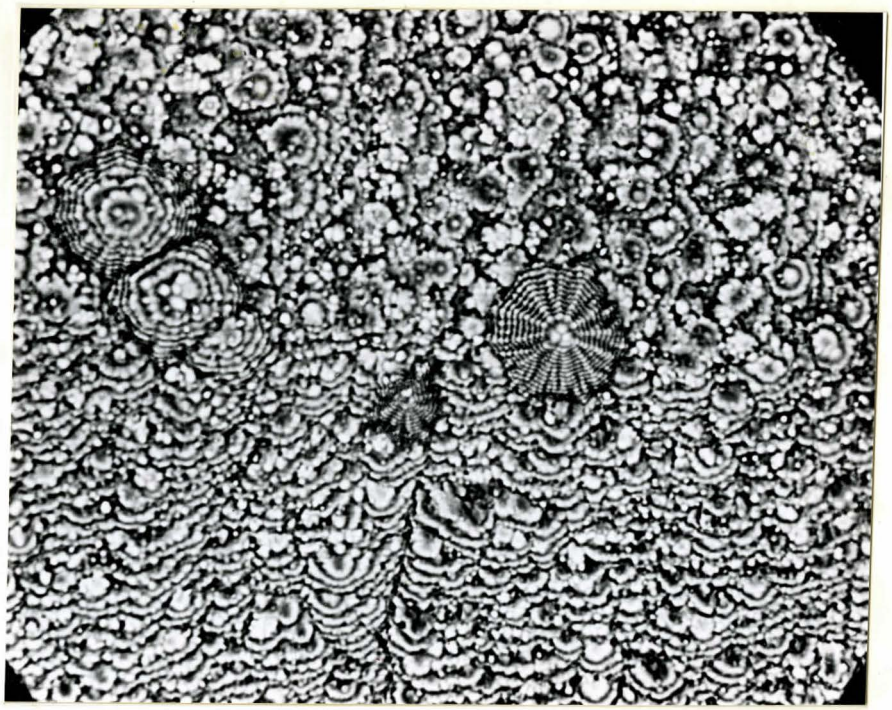

Fig. 1 (c) 900 sec. etch

0.5 Mm.

Scale for figures 1 and 2

FIGURE 2

0.24 Molar H Cl

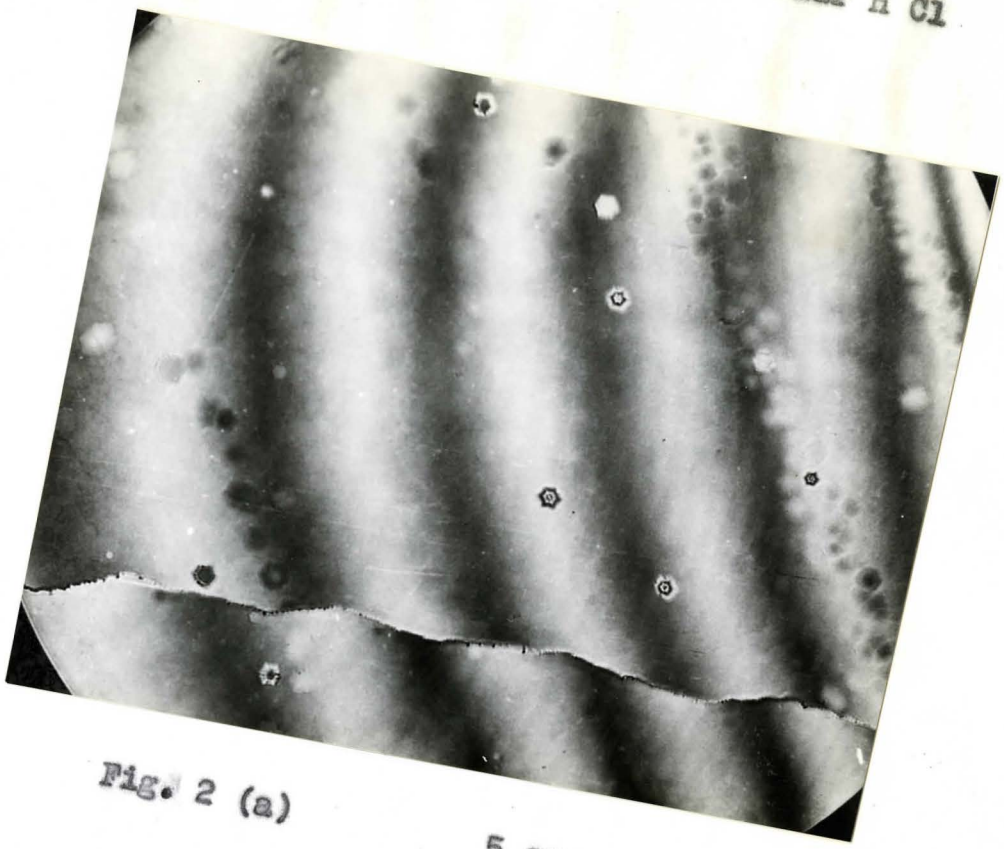

Fig. 2 (a)

5 sec. etch

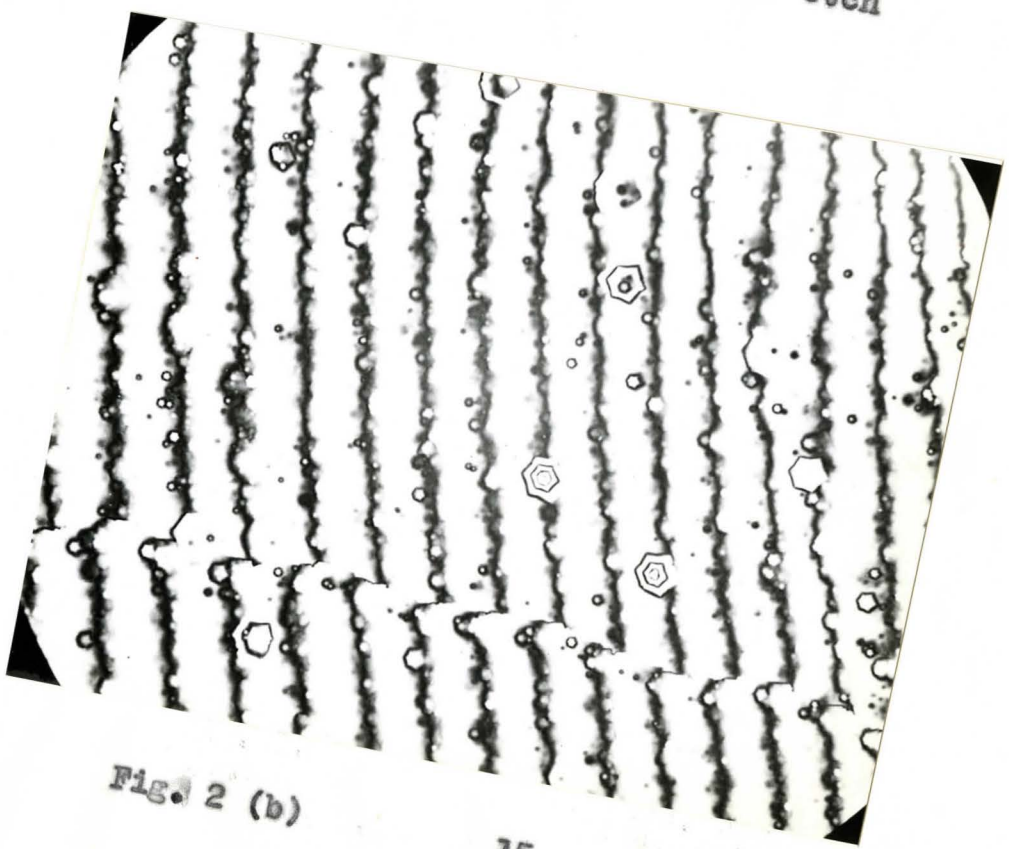

Fig. 2 (b)

15 sec. etch

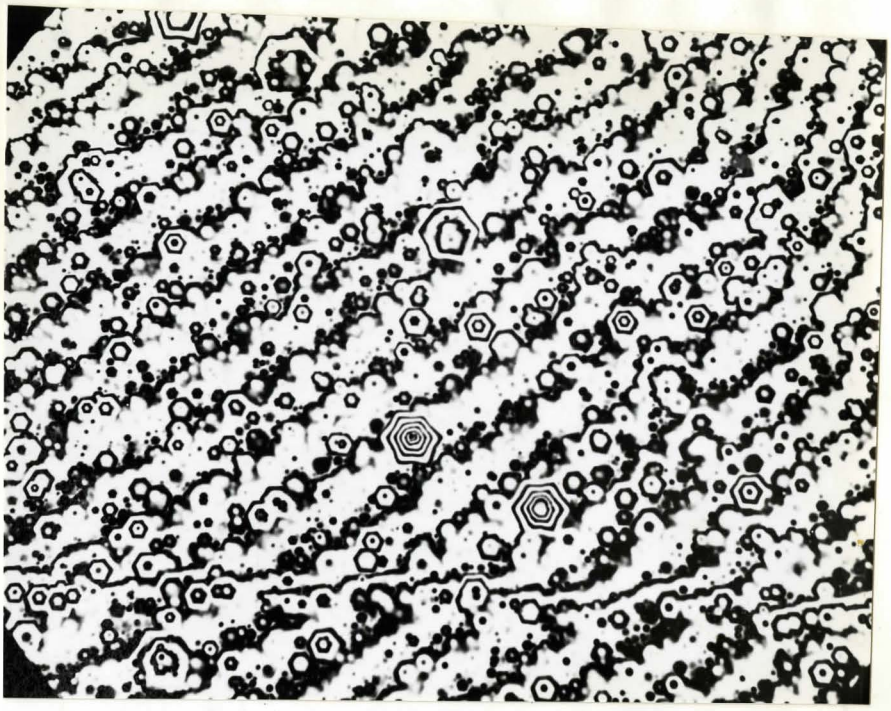

Fig. 2 (c) 40 sec. etch

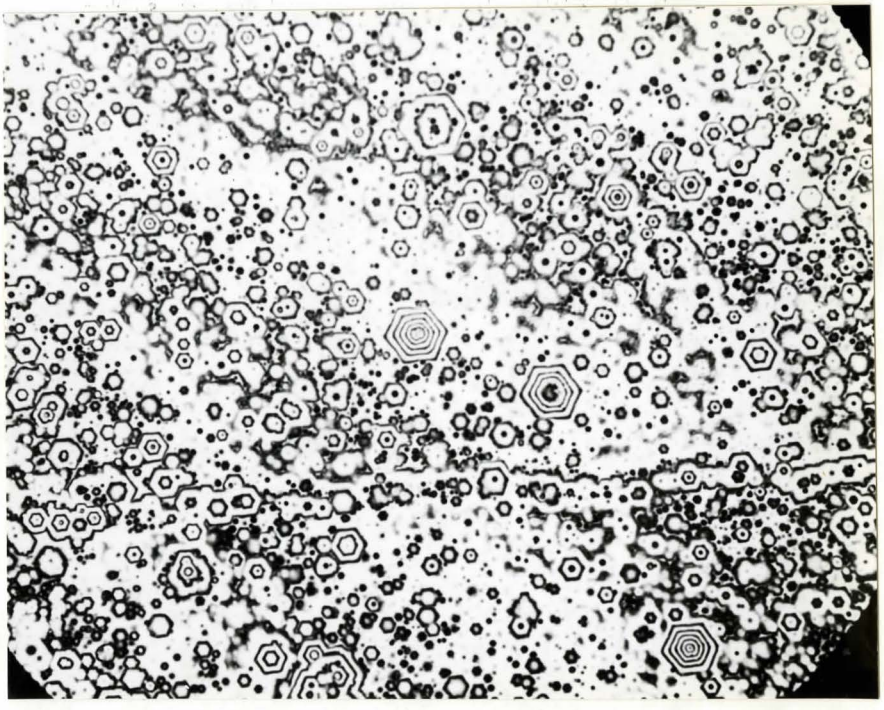

Fig. 2 (d) 60 sec. etch

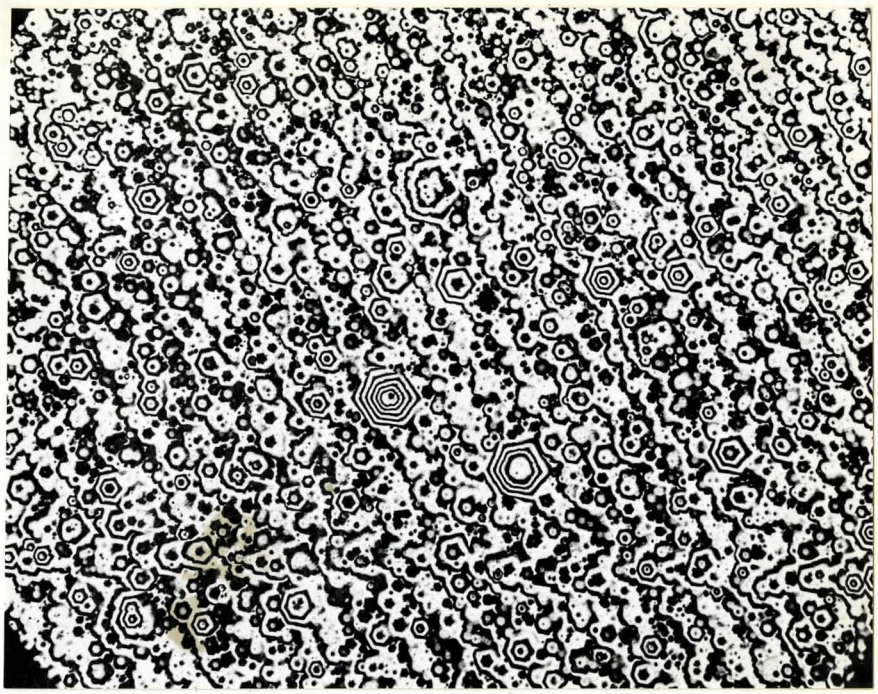

Fig. 2 (e) 75 sec. etch

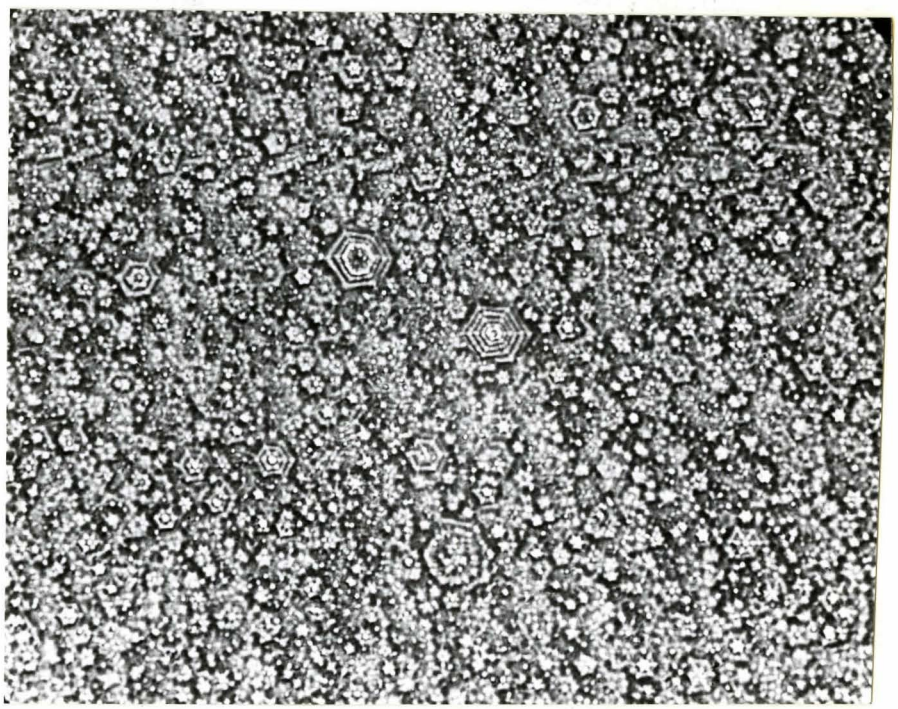

Fig. 2 (f) 90 sec. etch

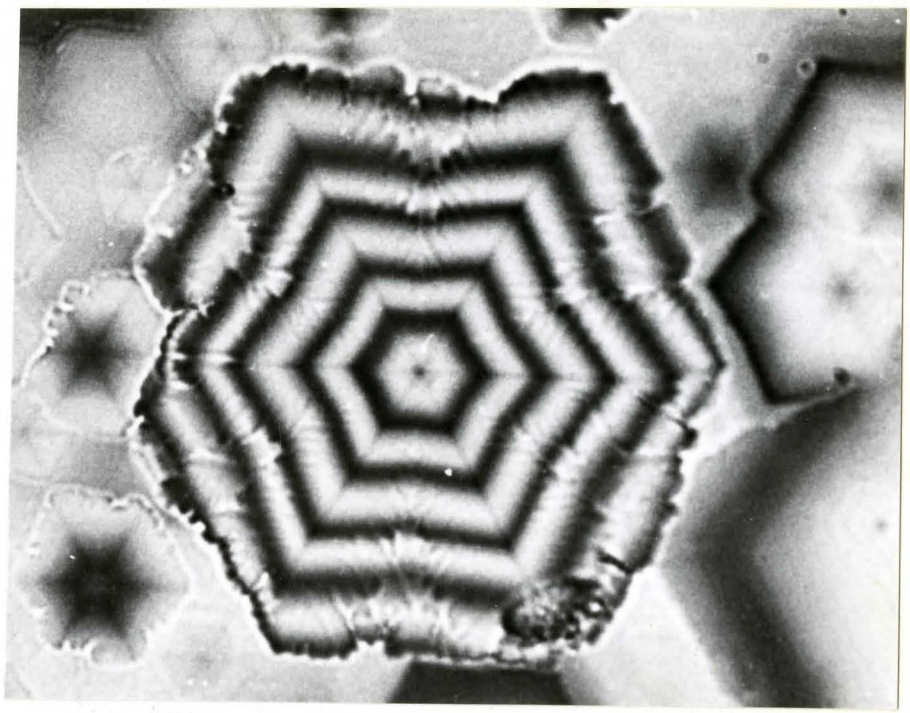

Fig. 3 120 sec. etch

0.3 Molar H Cl

Fig. 4 90 sec. etch
0.6 Molar H Cl

Fig. 5 45 sec. etch
1.2 Molar H Cl

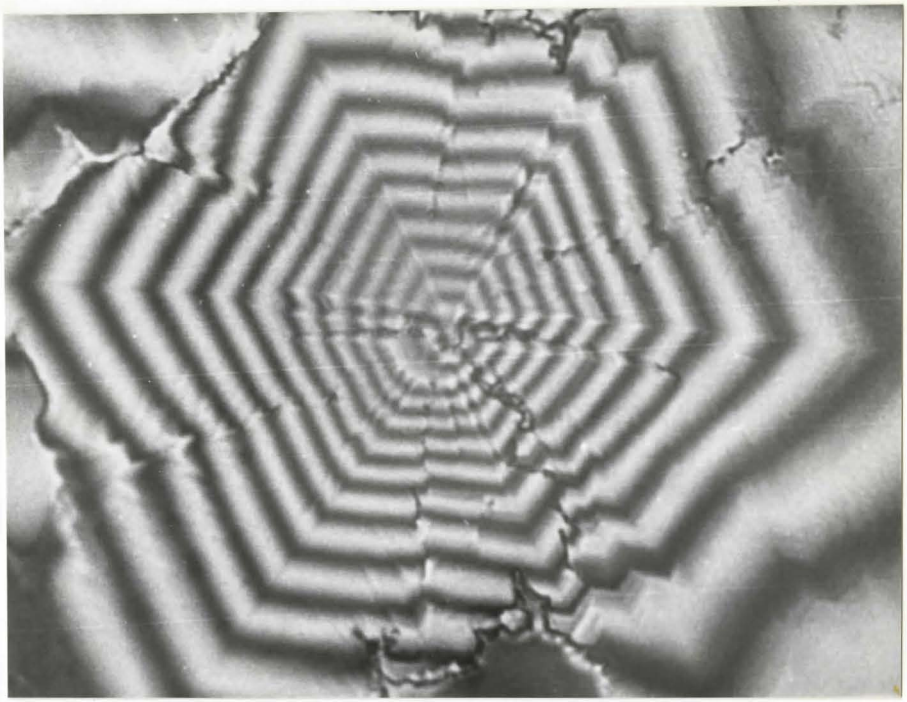

Fig. 6 30 sec. etch

1.2 Molar H Cl

Fig. 7 45 sec. etch
1.2 Molar H Cl

Fig. 8 45 sec. etch

2.4 Molar H Cl

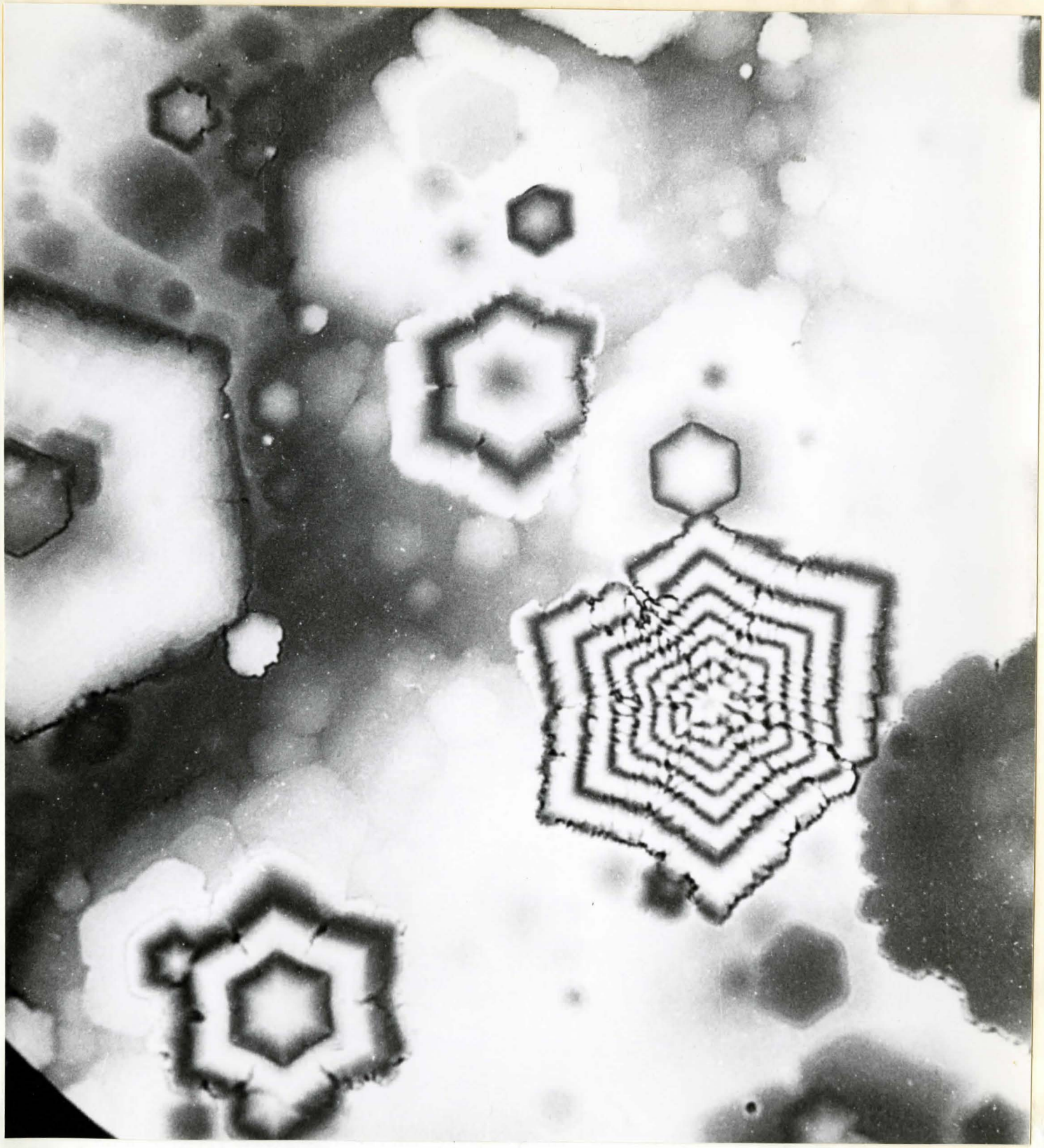

Fig. 9 90 sec. etch

0.3 Molar H Cl

Fig. 10 240 sec. etch

0.06 Molar H Cl

Fig. 11 45 sec. etch

2.4 Molar H Cl

Figure 12

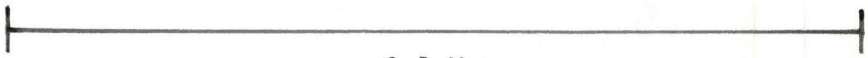

0.1 Mm.

Scale for figures 3 to 11

FIGURE 13

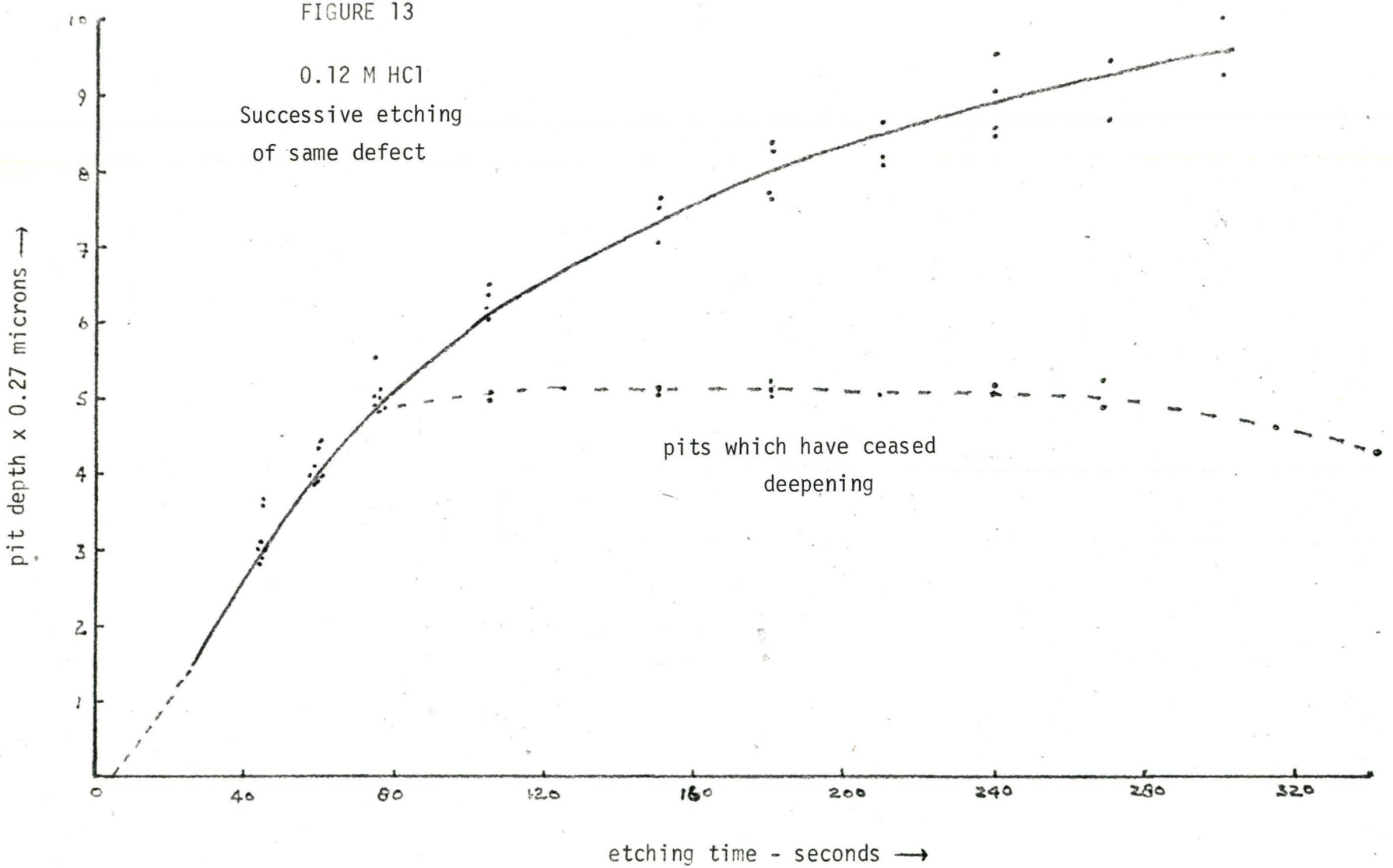
0.12 M HCl
Successive etching
of same defect
pits which have ceased
deepening
pit depth x 0.27 microns ⟶
etching time - seconds ⟶
0
40
80
120
160
200
240
280
320
1
2
3
4
5
6
7
8
9
10

FIGURE 14

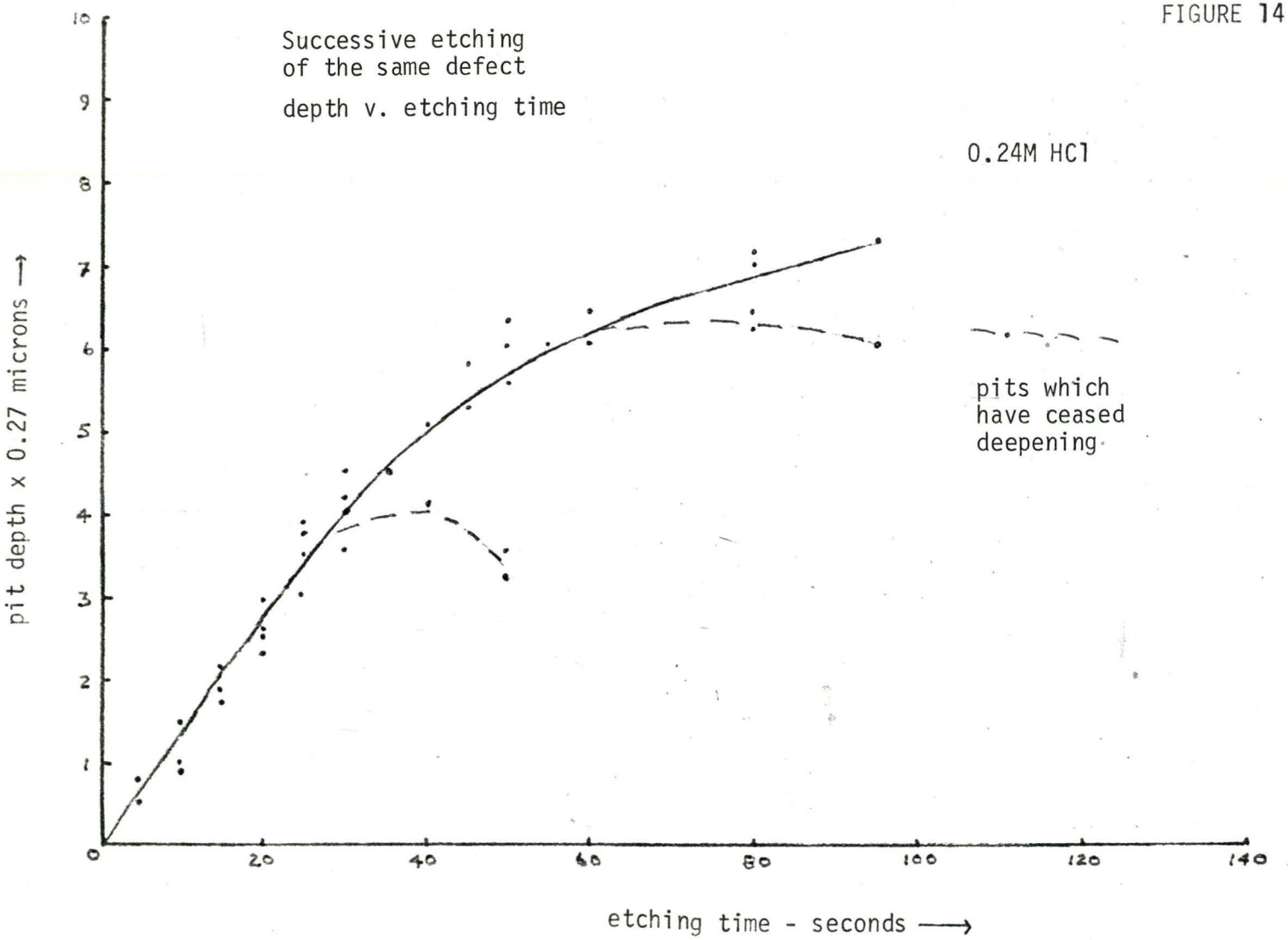
Successive etching
of the same defect
depth v. etching time
0.24M HCl
pits which
have ceased
deepening
pit depth x 0.27 microns ⟶
etching time - seconds ⟶
0
1
2
3
4
5
6
7
8
9
10
20
40
60
80
100
120
140

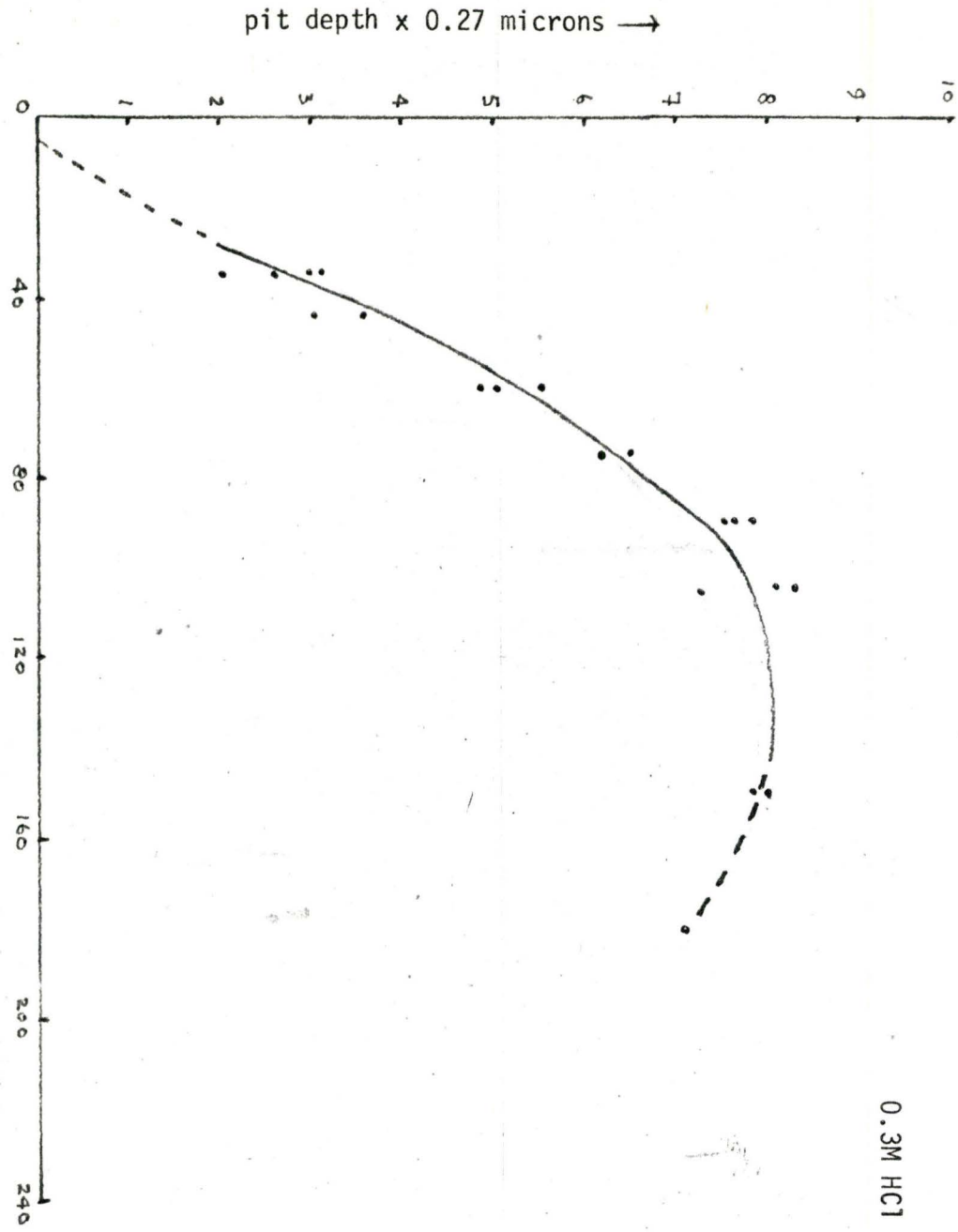

FIGURE 15

0.3M HCl

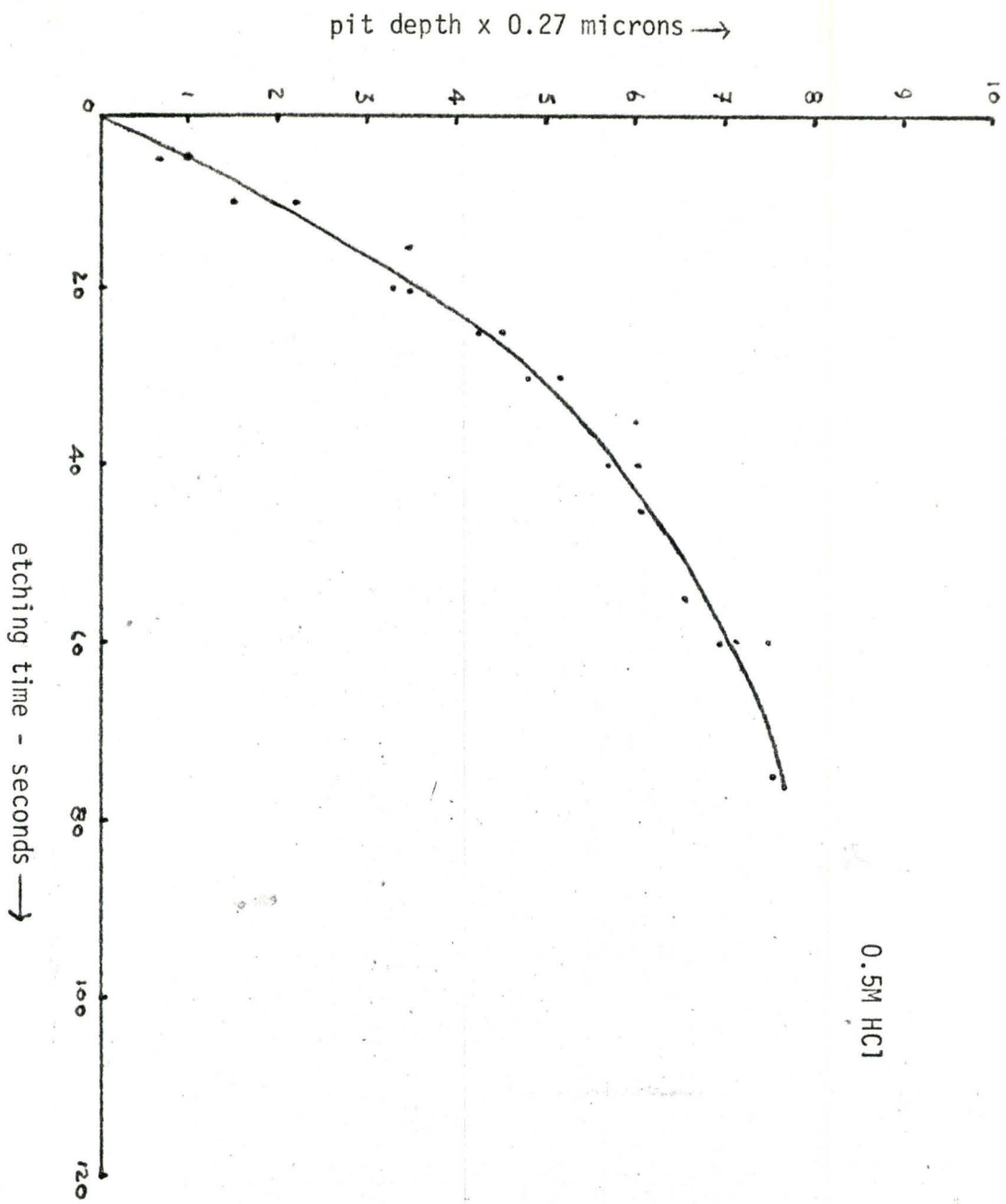

FIGURE 16

0.5M HCl

FIGURE 17

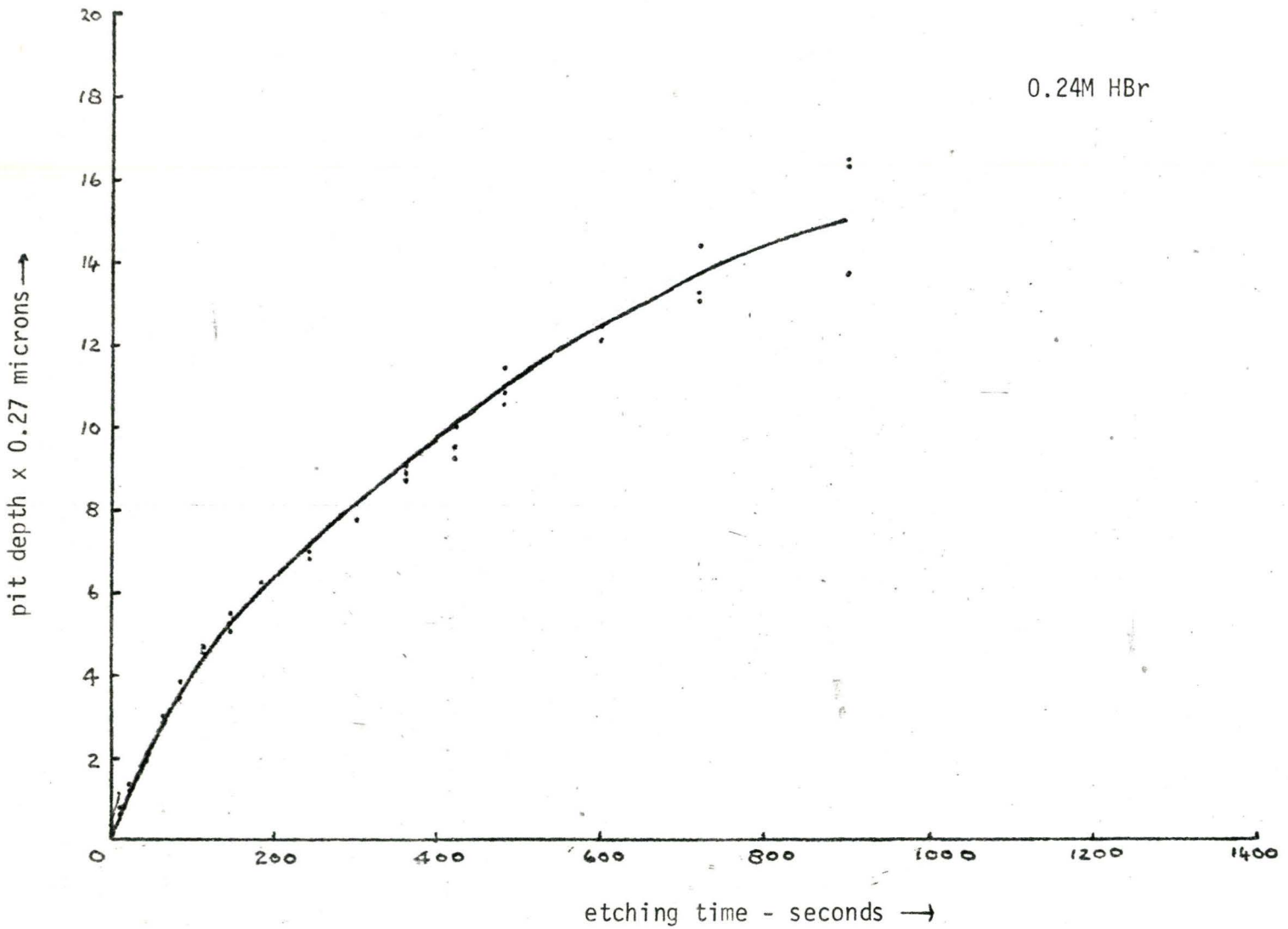
0.24M HBr
pit depth x 0.27 microns ⟶
20
18
16
14
12
10
8
6
4
2
0
200
400
600
800
1000
1200
1400
etching time - seconds ⟶

Figure 18

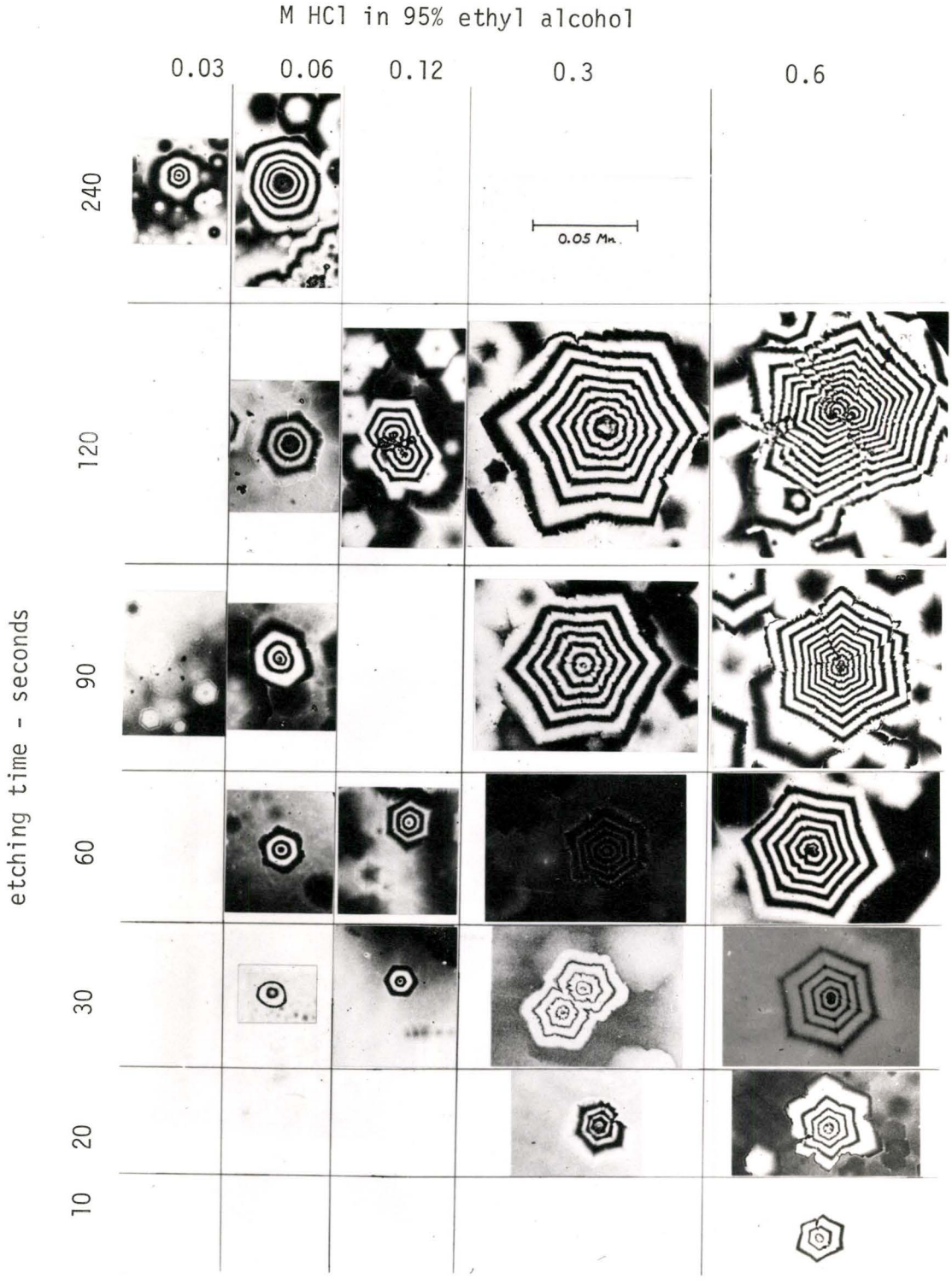
M HCl in 95% ethyl alcohol
0.03
0.06
0.12
0.3
0.6
240
120
90
60
30
20
10
etching time - seconds
0.05 Mn.

Figure 19

M HCl in 95% ethyl alcohol

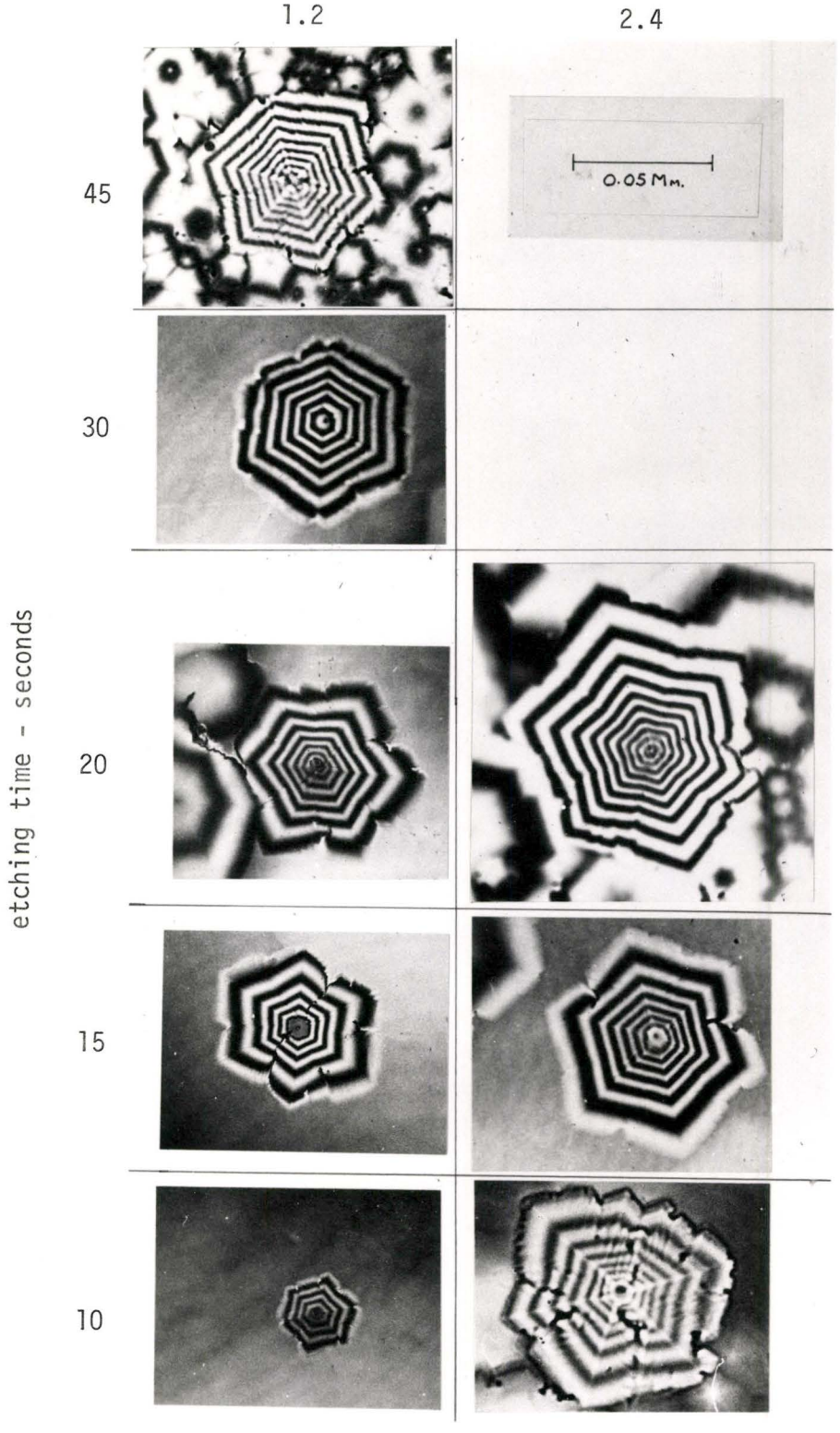

Table I

MHCl in 95% Ethyl Alcohol

etching time seconds	0.03		0.06		0.12		0.3	0.6	1.2		2.4
240	0.0262 9° 0.004		0.119 4.6° 0.01								
120			0.089 5.1° 0.008		0.116 7.2° 0.015	0.116 5.0° 0.010	0.256 4.1° 0.021	0.273 5.5° 0.025			
90	0.051 9° 0.008	0.082 11.5° 0.0165	0.084 7.6° 0.011				0.227 4.5° 0.022	0.288 5.9° 0.030			
60			0.152 4.0° 0.013	0.092 7.0 0.011	0.170 5.0° 0.014		0.296 4.9° 0.027	0.303 5.3° 0.028	0.405 6.0° 0.042		
30			0.119 4.6° 0.010		0.172 5.0° 0.014		0.332 6.0° 0.037	0.395 6.1° 0.038	0.620 5.7° 0.061		
20							0.424 7.0° 0.057	0.620 6.0° 0.065	0.871 6.0° 0.085		1.57 5.8° 0.160
15									1.14 4.6° 0.093		1.42 5.0° 0.121
10								0.615 7.2° 0.078	0.910 7.2° 0.108	1.80 4.6° 0.144	1.90 6.2° 0.200

$K' = d/t / \tan \theta$

θ' = mean true pit slope

d/t = rate of pit deepening μ/sec

etching time (seconds)

Table II

MHCl in 95% Ethyl Alcohol

etching time - seconds →	0.06	0.12	0.3		0.6		1.2	2.4
240	0.14		0.17					K'
	2.7°		2.1°					0'
	0.0066		0.0034					d/t
120	0.14	0.12	0.26	0.26	0.27	0.27		K'
	2.0°	2.3°	3.3°	2.5°	3.0°	2.2°		θ'
	0.005	0.0045	0.015	0.011	0.017	0.012		d/t
90					0.36			K'
					2.8°			0'
					0.018			d/t
60	0.16						0.405	K'
	2.5°						2.2°	0'
	0.0072						0.0108	d/t
45	K'							1.48
	0'							2.0
	d/t							0.048

Table III

MHCl in 95% Ethyl Alcohol

	0.06	0.12	0.3	0.6	1.2	2.4
240	0.13 1.3° 0.0029					
120	0.14 2.0° 0.0045		0.26 1.5 0.007	0.28 1.65° 0.0079		
90				0.34 1.5° 0.009		
60					0.41 1.6° 0.012	
45					1.05 1.6° 0.029	1.51 1.4° 0.035
30					1.13 1.6° 0.032	1.75 1.1° 0.037
20						2.1 1.5° 0.054
15						
10						3.8 1.4° 0.086

FIGURE 20

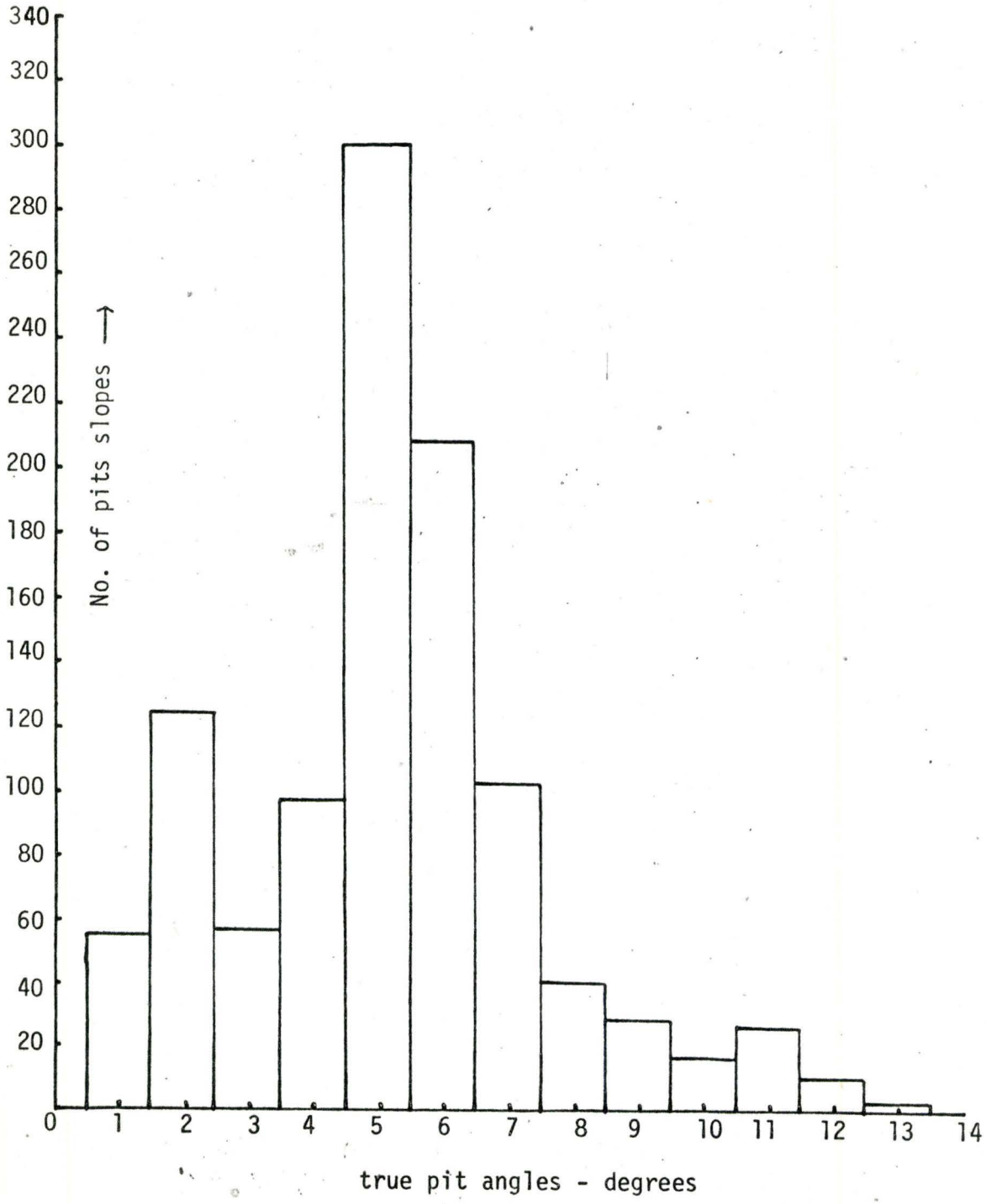
340
320
300
280
260
240
220
200
180
160
140
120
100
80
60
40
20
0
No. of pits slopes ⟶
1
2
3
4
5
6
7
8
9
10
11
12
13
14
true pit angles - degrees

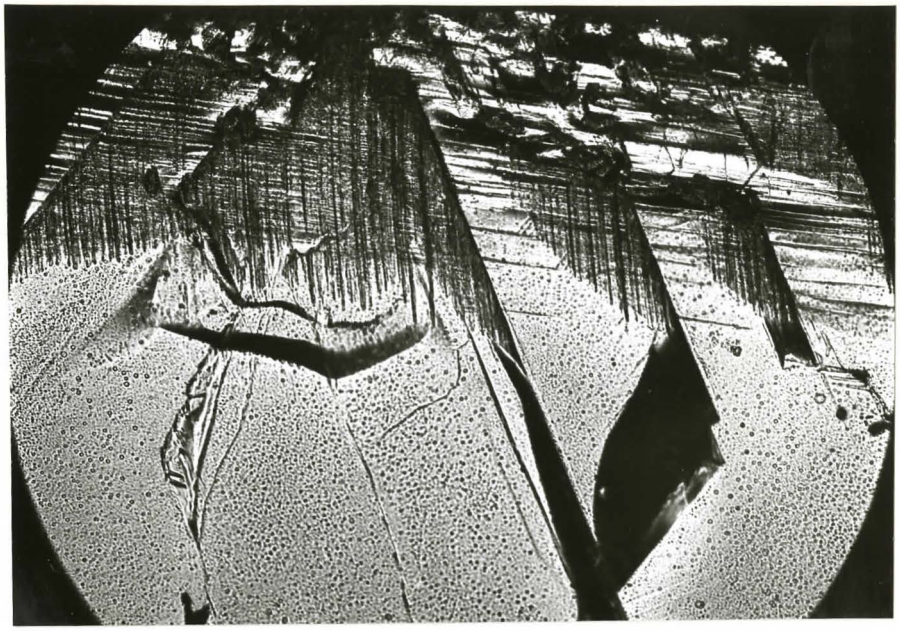

Figure 21

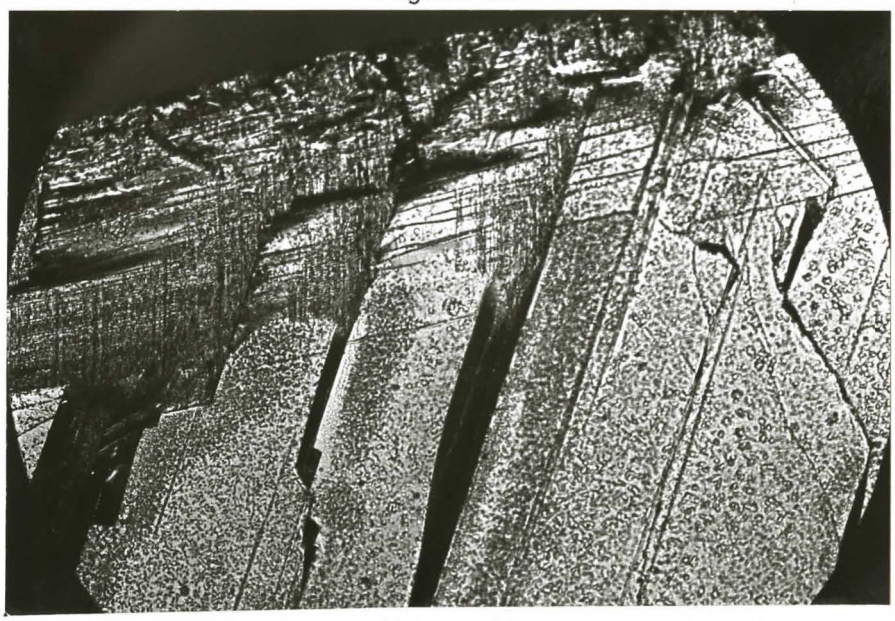

Figure 22

0.1 cm.

Scale for Figures 21 and 22.